# An intense terminal epoch of widespread fluvial activity on early Mars: 2. Increased runoff and paleolake development

Rossman P. Irwin III,[1] Alan D. Howard,[2] Robert A. Craddock,[1] and Jeffrey M. Moore[3]

Received 15 April 2005; revised 16 September 2005; accepted 21 September 2005; published 2 December 2005.

[1] To explain the much higher denudation rates and valley network development on early Mars (>~3.6 Gyr ago), most investigators have invoked either steady state warm/wet (Earthlike) or cold/dry (modern Mars) end-member paleoclimates. Here we discuss evidence that highland gradation was prolonged, but generally slow and possibly ephemeral during the Noachian Period, and that the immature valley networks entrenched during a brief terminal epoch of more erosive fluvial activity in the late Noachian to early Hesperian. Observational support for this interpretation includes (1) late-stage breaching of some enclosed basins that had previously been extensively modified, but only by internal erosion and deposition; (2) deposition of pristine deltas and fans during a late stage of contributing valley entrenchment; (3) a brief, erosive response to base level decline (which was imparted as fretted terrain developed by a suite of processes unrelated to surface runoff) in fluvial valleys that crosscut the highland-lowland boundary scarp; and (4) width/contributing area relationships of interior channels within valley networks, which record significant late-stage runoff production with no evidence of recovery to lower-flow conditions. This erosion appears to have ended abruptly, as depositional landforms generally were not entrenched with declining base level in crater lakes. A possible planetwide synchronicity and common cause to the late-stage fluvial activity are possible but remain uncertain. This increased activity of valley networks is offered as a possible explanation for diverse features of highland drainage basins, which were previously cited to support competing warm, wet and cold, dry paleoclimate scenarios.

**Citation:** Irwin, R. P., III, A. D. Howard, R. A. Craddock, and J. M. Moore (2005), An intense terminal epoch of widespread fluvial activity on early Mars: 2. Increased runoff and paleolake development, *J. Geophys. Res.*, *110*, E12S15, doi:10.1029/2005JE002460.

## 1. Introduction

[2] Like most extraterrestrial surfaces, the Martian highlands preserve a record of intense early impact bombardment, which declined over the first ~800 Myr after accretion (absolute age estimates herein follow *Hartmann and Neukum* [2001]). On Mars, however, volatile-driven erosion processes significantly modified the oldest impact craters (Figure 1a), and craters <30 km wide were preferentially removed from the surface record [e.g., *Öpik*, 1966; *Arvidson*, 1974; *Neukum and Hiller*, 1981; *Strom et al.*, 1992; *Grant and Schultz*, 1993; *Craddock et al.*, 1997; *Forsberg-Taylor et al.*, 2004]. This intense crater degradation and burial occurred simultaneously with valley network development, primarily during the Noachian Period, prior to ~3.7 Ga. The contemporary heavy impact flux disrupted drainage basins as they were forming [*Carr and Clow*, 1981; *Irwin and Howard*, 2002], creating new enclosed intercrater and intracrater basins where sediment accumulated and where ponding may have occurred. Superimposed fresh crater populations indicate that valley network activity declined during the Late Noachian to Early Hesperian Epochs [*Tanaka*, 1986; *Craddock and Maxwell*, 1990, 1993; *Irwin and Howard*, 2002; *Irwin et al.*, 2004a], and Mars presently has negligible wind-dominated denudation rates on all but the most friable surfaces [*Golombek and Bridges*, 2000; *Grant et al.*, 2005].

[3] Many investigators have debated the potential for valley network development in end-member warm, wet (modern Earth) or cold, dry (modern Mars) paleoclimate scenarios [e.g., *Sagan et al.*, 1973; *Pieri*, 1980; *Goldspiel and Squyres*, 2000; *Gulick*, 2001; *Craddock and Howard*, 2002; *Gaidos and Marion*, 2003]. The warm, wet scenario is founded primarily on indications that precipitation runoff, which does not occur in the thin, cold modern atmosphere, was responsible for valley networks and impact crater degradation. Some tributaries head near sharp ridge crests where large upslope aquifers are not available (Figure 1b) [*Milton*, 1973; *Masursky et al.*, 1977; *Irwin and Howard*, 2002; *Craddock and Howard*, 2002; *Hynek and Phillips*, 2003; *Stepinski and Collier*, 2004], Noachian impact craters in the equatorial highlands exhibit morphologic and mor-

[1]Center for Earth and Planetary Studies, National Air and Space Museum, Smithsonian Institution, Washington, D. C., USA.
[2]Department of Environmental Sciences, University of Virginia, Charlottesville, Virginia, USA.
[3]Space Sciences Division, NASA Ames Research Center, Moffett Field, California, USA.


0148-0227/05/2005JE002460$09.00

phometric properties that are most consistent with fluvial degradation [*Craddock and Maxwell*, 1993; *Craddock et al.*, 1997; *Forsberg-Taylor et al.*, 2004], and recharge was necessary to support the erosion of valley network volumes [*Howard*, 1988; *Goldspiel and Squyres*, 1991; *Grant*, 2000; *Gulick*, 2001; *Craddock and Howard*, 2002]. Crater degradation and loss of small craters were ubiquitous in the Noachian highlands, not restricted to valley floors where groundwater would have preferentially emerged and collected (Figures 1 and 2). The width of channels in Martian valley networks increases with contributing area as is observed in terrestrial drainage basins, suggesting at least episodic, localized runoff production rates on the order of a few centimeters per day, well above reasonable base flow conditions [*Irwin et al.*, 2005].

[4] In two important respects, degraded craters in the equatorial highlands of Mars are distinct from lunar and Mercurian analogs. First, degradation has resulted in both rim lowering and basin infilling on all three bodies, but on Mars the erosive processes consistently yielded an abrupt concave break in slope that separates gullied crater sidewalls from a low-gradient interior deposit (Figure 1). This feature is not consistent with the smoothly concave interiors and rounded rims that are characteristic of diffusive cratering or of mass wasting by diffusional creep [*Craddock et al.*, 1997; *Craddock and Howard*, 2002; *Forsberg-Taylor et al.*, 2004]. Second, on the Moon and Mercury, younger small craters were responsible for much of the degradation of older craters, whereas on Mars, small craters were removed from the surface population at the same time that larger craters were eroded. For these reasons, cratering and mass wasting were not the main mechanisms that were responsible for Martian crater degradation. Wind has not significantly modified the large Martian craters that have formed since the Noachian [*Craddock et al.*, 1997], and its earlier effectiveness would depend on atmospheric density and a suite of weathering processes that could produce sediment more rapidly than it was trapped (mobile sand supply limits modern aeolian abrasion at Gusev crater [*Grant et al.*, 2005]). Basaltic volcanism cannot explain the observed rim modification of the old craters or the ubiquitous small crater loss on both high- and low-standing surfaces. These observations leave slow or ephemeral fluvial processes as the only reasonable mechanism for the erosion of Martian craters [*Craddock and Howard*, 2002].

[5] A number of observations have been cited in support of geothermal water sources in a cold, dry paleoclimate: the theater-headed morphology of many valleys (Figure 2), the undissected or poorly dissected areas between valleys (Figures 1b and 2) [*Pieri*, 1980; *Baker*, 1982, p. 57; *Mars Channel Working Group*, 1983; *Malin and Carr*, 1999; *Gulick*, 2001], the generally immature development of Martian drainage basins, and the infrared spectral signatures of basalt and dust rather than chemical weathering products in most highland regions [*Bandfield et al.*, 2000, 2003]. Although *Mangold et al.* [2004] reported localized drainage density measurements up to 1.5 km/km$^2$, the common scarcity of incised low-order tributaries on Mars generally yields drainage density measurements on the order of $\sim 10^{-1}$ to $10^{-2}$ km/km$^2$ or less. This value is orders of magnitude higher than the density of lunar or Venusian volcanic rilles, but an order of magnitude or more below common terrestrial drainage densities [*Baker and Partridge*, 1986; *Grant and Schultz*, 1993; *Carr and Chuang*, 1997; *Grant*, 2000; *Cabrol and Grin*, 2001a; *Irwin and Howard*, 2002; *Hynek and Phillips*, 2003; *Stepinski and Collier*, 2004]. Studies of impact crater degradation suggest past denudation rates that are comparable to those of some terrestrial desert or periglacial climates [*Craddock and Maxwell*, 1993; *Carr*, 1996, p. 135; *Craddock et al.*, 1997]. Many highland basins remain enclosed despite past fluvial activity, and valleys are therefore commonly short [*Carr and Clow*, 1981; *Irwin and Howard*, 2002], although some valleys or systems of interconnected basins extend over 1000 km in length. Terrestrial watersheds that have been fully regraded by runoff are concave in longitudinal profile, planform, and cross-section, but the topography of Martian drainage basins is generally not consistent with this mature form [*Aharonson et al.*, 2002; *Luo*, 2002; *Stepinski and Coradetti*, 2004; *Stepinski et al.*, 2004]. *Pieri* [1980] used planimetric analysis without the benefit of topographic data to show that Martian low-order tributaries are often subparallel and enter higher-order reaches at unpredictable junction angles, suggesting that precursor topography still largely controls Martian network planform. In mature terrestrial drainage basins, the junction angle between a low- and high-order tributary is greater than the angle between two tributaries of comparable order, which is related to the predictable decline in longitudinal gradient with distance from the stem valley head [*Horton*, 1932; *Howard*, 1971]. A distinction must be made between features that could reflect competing processes or drainage basin immaturity, like those mentioned above, from characteristics that would be unique to groundwater sapping. Finally (and perhaps most critically), paleoclimate models have difficulty producing a warm, wet environment given the presumably fainter young Sun (see reviews by *Squyres and Kasting* [1994], *Haberle* [1998], *Carr* [1999], and *Craddock and Howard* [2002]). *Graedel et al.* [1991] and *Whitmire et al.* [1995] discuss the concept of early stellar mass loss, whereby the early Sun may have been more luminous than is generally supposed. Results from one observational test support the concept, but although the resulting higher irradiance helps, it may be inadequate to produce a warm early Mars by itself [*Gaidos et al.*, 2000]. *Colaprete et al.* [2005] present a model whereby water vapor released by impacts supplements the $CO_2$ greenhouse of a thicker early atmosphere, temporarily raising temperatures above freezing and allowing precipitation and runoff to occur. Some combination of these influences may have been responsible for warmer, wetter periods of time on early Mars.

[6] Given the evidence cited above for ubiquitous erosion on Noachian Mars and the role of precipitation in the development of valley networks, one of the most important outstanding questions is how the Noachian craters became so deeply degraded while the valley networks remained poorly developed. *Grant* [1987, 2000] suggested an intermediate concept wherein precipitation-recharged groundwater sapping was the dominant process in valley network development. His model is appealing in that it may explain both the theater-headed valleys on intercrater plains and the denser upslope tributaries that originate near drainage divides, and it has a sound terrestrial analog, but the requirement for infiltration requires a thawed surface layer

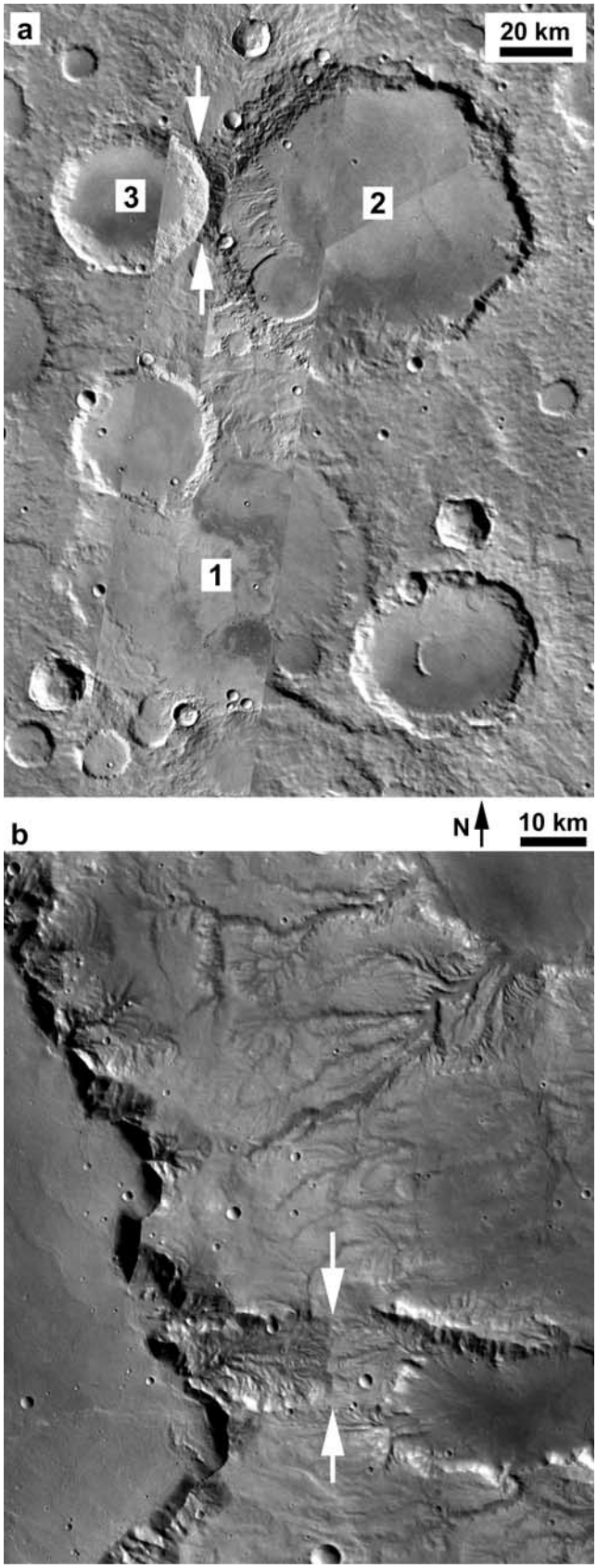


and therefore long-term, higher mean temperatures than would a mechanism that relies entirely on runoff. *Baker and Partridge* [1986] observed that some Martian valley networks have pristine V-shaped cross-sections in their downstream reaches, with more degraded upstream reaches that have flat floors and crenulated or gullied sidewalls. Their scenario has runoff and sediment derived from upslope in early stages, whereas later erosion at lower altitudes relied on groundwater. *Grant* [1987] and *Grant and Schultz* [1990] also proposed discrete stages of valley network development or landscape gradation, some occurring during the Hesperian, based on the stratigraphy and crater retention ages of geologic units.

[7] *Irwin and Howard* [2002] discussed the role of concomitant impact cratering in disrupting Martian valley networks, through direct burial by ejecta, damming of flow paths, and regrading due to base level changes in the terminal basin. Ongoing large impacts maintained the multibasin landscape at scales of tens to hundreds of kilometers, thereby inhibiting drainage integration to some extent, but denudation was still adequate to fill and reduce the population of many craters <30 km in diameter (relative to the Moon, Mercury, and later Mars) through the Middle and Late Noachian Epochs, over a time of 200 million years or more [*Craddock and Maxwell*, 1990, 1993]. It is therefore unlikely that cratering alone explains the immaturity of Martian valley networks on the kilometer scale. Landscape denudation on the order of hundreds of meters, which is required to explain degraded crater morphometry

**Figure 1.** (a) Adjacent impact craters in diverse states of degradation, centered at 18.2°S, 148.5°E in Terra Cimmeria. The sequence of impacts is 1, 2, 3. Superimposed craters (such as 3 over 2) are generally less degraded than are the underlying craters, unless the superimposed craters are much smaller. Larger craters would require a longer time for degradation, so the less advanced degradation of the smaller, superimposed crater 3 demonstrates that landscape degradation was occurring both before and after the crater 3 impact. Similarly, crater 1 is more degraded and therefore likely older than crater 2 despite their similar size. From this relationship, which is observed across the cratered highlands, crater degradation is thought to have been a slow but long-term process. A Noachian/Hesperian boundary population of superimposed fresh craters attests to the nearly complete decline of crater degradation around 3.7 billion years ago, and more recent aeolian processes have been ineffective at modifying these large craters [*Craddock and Maxwell*, 1990, 1993; *Irwin and Howard*, 2002]. Gullies are developed on both sides of the narrow ridge between 2 and 3 (white arrows). THEMIS daytime IR/Viking Mars Digital Image Mosaic (MDIM) 2.1 overlay. (b) Valley networks on the eastern rim of Huygens crater in Terra Tyrrhena, centered at 13.4°S, 60.2°E. Valley networks are denser on steep slopes and extend to the crests of sharp ridges, where they occur (e.g., white arrows). Where interfluves are undissected, networks had insufficient time to regrade the landscape to a set of space-filling, concave drainage basins. Although crater degradation was a ubiquitous process, valley network development remained immature. Mars Express High Resolution Stereo Camera image (orbit 532), ESA/DLR/FU Berlin.

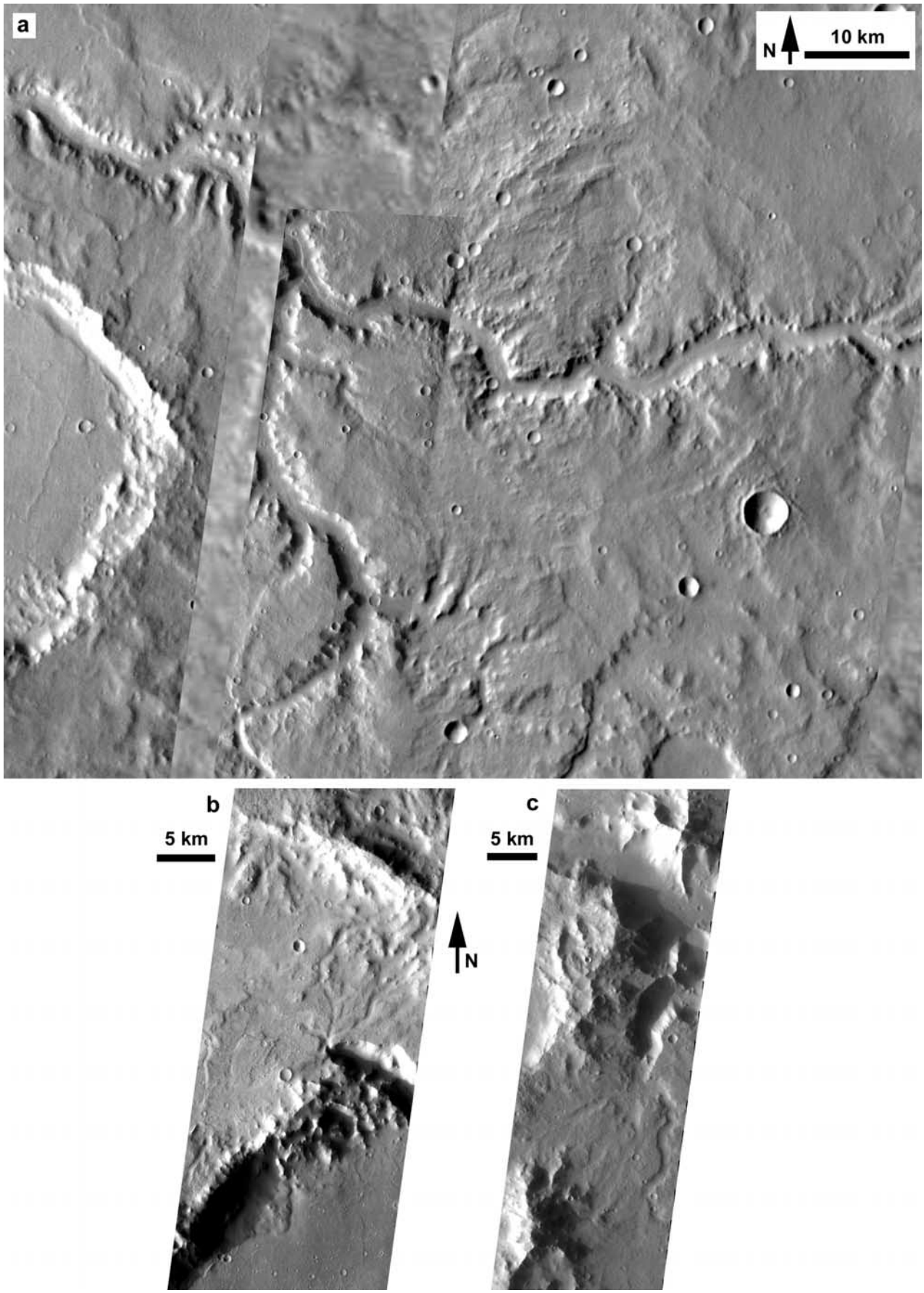


**Figure 2**

[*Craddock and Maxwell*, 1993; *Craddock et al.*, 1997], would occur on Earth in 10 million years or less at the terrestrial average rate of 65 m/Myr [*Knighton*, 1998, p. 81], and valley networks like those on Mars (typically ~1 km wide by ~50–350 m deep) would take even less time to form on Earth. Despite this observation, the often great diversity in degradation state between adjacent impact craters of similar size (Figure 1a) requires that crater degradation was a long-term process. For these reasons we infer that Noachian erosion was slow by terrestrial standards, and that warmer, wetter episodes or epochs must have been either short-lived or inefficient at producing runoff.

[8] In this and a companion paper [*Howard et al.*, 2005], we discuss observational evidence that the relict valley networks developed during an epoch of enhanced fluvial erosion in the Late Noachian to Early Hesperian, relative to conditions that prevailed earlier in the Noachian when much of the crater degradation occurred. The later stage of fluvial activity was generally more intense than was the suite of geomorphic processes that operated earlier in the Noachian, but it was shorter-lived and therefore less effective in its totality. Knickpoint development and basin piracy during this late phase can explain some features that were previously attributed to groundwater sapping. Support for this concept comes from (1) entrenchment and extension of valley networks into older erosional and depositional surfaces, which had sustained considerable degradation and loss of craters without developing mature drainage basins [*Howard et al.*, 2005]; (2) late-stage breaching of some enclosed basins that previously had been substantially modified, but only by internal erosion and deposition; (3) development of pristine, undissected deltas during a late stage of contributing valley entrenchment; (4) a brief, incomplete response of valley longitudinal profiles to base level decline along the highland/lowland boundary scarp, which was imparted by fretted and knobby terrain development by non-fluvial processes; and (5) relationships between width and contributing area of interior channels within valley networks, which indicate significant (Earth-like) runoff production rates with no evidence of recovery to lower-flow conditions. These landforms record the final stage of fluvial activity in their respective drainage basins during the Late Noachian to Early Hesperian Epochs, but the precise timing of these local events relative to each other and to the global stratigraphic scheme remains to be established. This scenario is a potential explanation for many features on Mars that were previously cited in support of disparate climate models; however, detailed analyses of a large number of drainage basins are necessary to test and refine this concept.

## 2. Late-Stage Breaching of Enclosed Basins

[9] Many basins on Mars have entrance and/or exit breaches that are associated with valley networks. Some crater rim breaches are fairly pristine and V-shaped in cross-section, suggesting active downcutting of the inlet or outlet valley near the end of fluvial activity, with little or no subsequent gullying or retreat of the valley sidewalls. Here we discuss type examples of three related landforms: the pristine entrance breach (section 2.1); the pristine exit breach (section 2.2); and the entrenchment of an outlet valley floor, leaving valley wall terraces (section 2.3). Finally, we briefly describe a long valley network in Arabia Terra and Terra Sabaea, which appears to have extended downslope during late-stage overflow of several previously enclosed but highly degraded basins (section 2.4). All of these basins preserve evidence of late-stage, abundant runoff from highland valley networks, and depositional landforms or narrow outlet valleys suggest that runoff-fed paleolakes occupied many of these basins during this late epoch of flow.

### 2.1. Pristine Entrance Breach: Gale Crater

[10] Gale crater has a diameter of 155 km and is located along the crustal dichotomy boundary in Terra Cimmeria (5°S, 138°E). *Cabrol et al.* [1999] suggested that Gale contained a paleolake up to at least the northern crest of the crater rim, primarily on the basis of two features: a layered, terraced, central mound; and the (sparse) fluvial dissection of the mound and crater rim, including a significant entrance breach in the relatively highstanding southern side of the rim (Figure 3). *Greeley and Guest* [1987] mapped the interior mound and interpreted it as "interbedded lava flows and sedimentary deposits of aeolian or fluvial origin." *Pelkey and Jakosky* [2002] and *Pelkey et al.* [2004] presented a detailed analysis of imaging and thermophysical data for Gale crater, focusing on the nature of its geologic materials. The mound is likely of sedimentary origin given its susceptibility to aeolian deflation, as shown by the abundant yardangs on its surface, and it may have originally been more areally extensive [*Malin and*

**Figure 2.** Features of Martian valley networks are more consistent with a brief, late-stage epoch of surface runoff than with a longer period of groundwater sapping. (a) Naktong Vallis (centered at 0°N, 37°E, Terra Sabaea/Arabia Terra) is incised into an older basin surface, which is now preserved as poorly dissected interfluves between the main tributary branches. Small tributaries originate on the interfluve surface rather than at headwalls within the valley, but the convex longitudinal profiles of these tributaries suggest rapid downcutting of the main valley (which has a much larger contributing area and therefore discharge; see section 2.4) relative to tributary incision rates. (b) The late-stage overflow and breaching of a crater rim at the lower side of this frame (by rim erosion along with infilling of the upper basin) created a sudden decline of base level for drainage within the upper basin. Headward propagation of a knickpoint can produce a theater-headed lower reach that is very similar in form to valleys carved by groundwater sapping. However, upslope tributaries are evident in the new high-resolution imaging, so sapping is not the sole cause for the theater head, and it may not have played a role at all. The absence of similar incised valleys around the rest of the crater supports the overland flow knickpoint concept. THEMIS V06500001, 6.28°S, 130.4°E (Terra Cimmeria), 18.4 km across. (c) Headward propagation of tributary knickpoints off the wide northern valley discussed in section 2.2 may have also produced this theater-headed lower reach with upslope tributaries. THEMIS V06523001, 13.76°S, 173.83°W (Terra Sirenum), 17.9 km across.

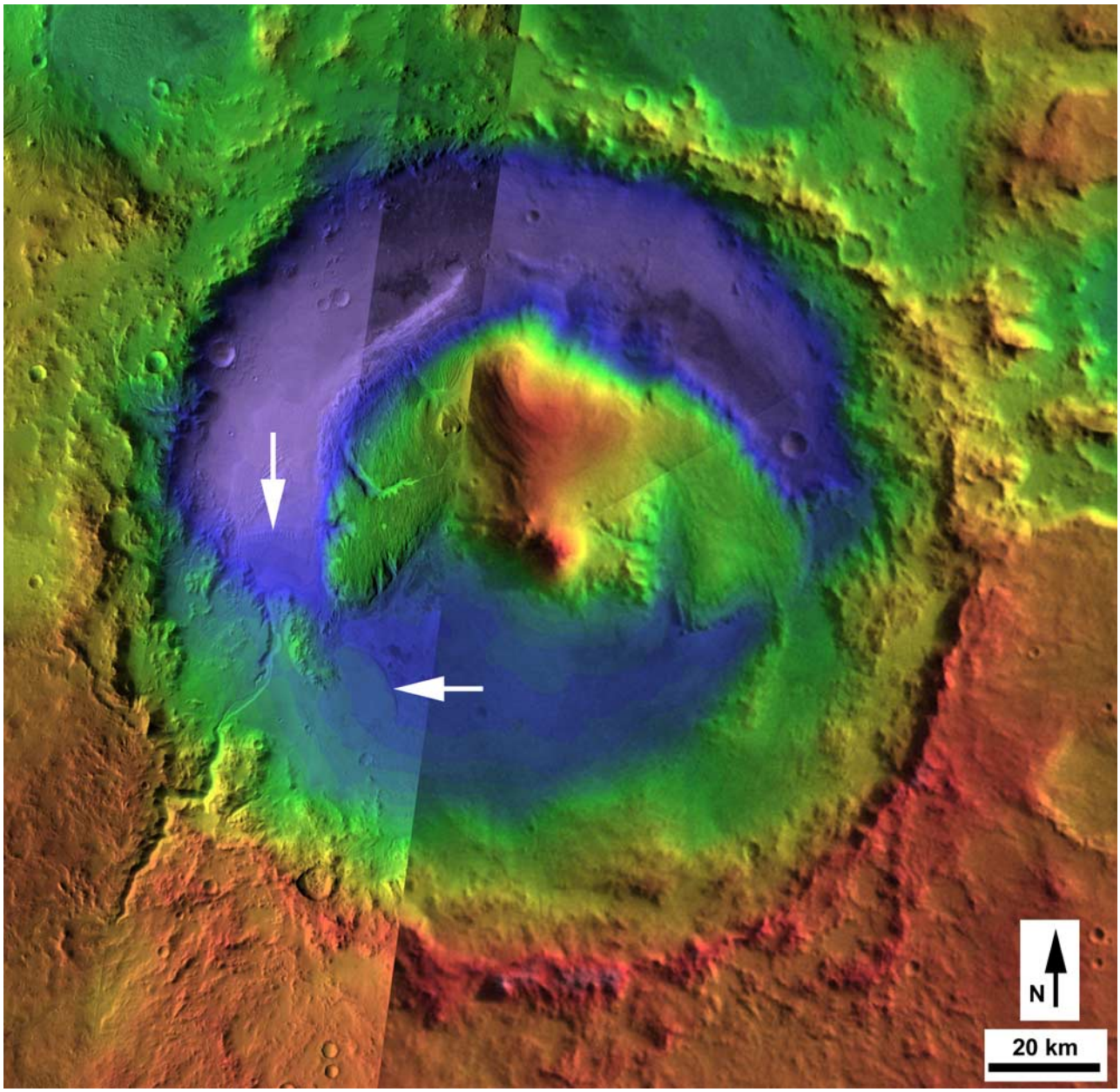


**Figure 3.** Detail of Gale crater (5°S, 138°E, 155 km diameter), in a mosaic of Viking Orbiter MDIM 2.1 and THEMIS daytime IR imaging, colorized with MOLA topography as in Figure 4. Note the rugged rim of the crater, the northward tilt of the rim, the central layered mound that is streamlined in response to winds from the north, the single entrance breach from the southwest, and the poor development of gullies on the interior wall and on the mound. White arrows give the location of scarp-fronted deposits discussed and displayed in greater detail in section 3. The dominant aeolian erosion of this mound prior to incision of its gullies and the confinement of two separate deltas on either side of the central mound at different elevations suggest a hiatus in valley network activity while the crater was buried and the interior mound was sculpted by wind.

*Edgett*, 2000; *Edgett and Malin*, 2001]. The mound is arcuate in plan view in response to winds from the north, which also dominate the dune transport in the region [*Pelkey et al.*, 2004]. Here we elaborate on the crater's age, stratigraphic position, and degradation, which suggest a hiatus between discrete episodes of erosive, late-stage valley network activity.

[11] Gale crater is adjacent to the Aeolis and Nepenthes Mensae fretted and knobby terrains (Figure 4a), which provide an important stratigraphic marker for dating the crater. *Irwin et al.* [2004b] argued that Aeolis Mensae formed in a thick sedimentary deposit (previously mapped as the "plateau" [*Scott et al.*, 1978] or "subdued cratered" unit [*Greeley and Guest*, 1987]) that was emplaced against the older crustal dichotomy boundary after fluvial activity had largely declined. This conclusion was based on the fretted and knobby terrains' boulder-free talus (at a resolution of meters), susceptibility to aeolian deflation (yardangs,

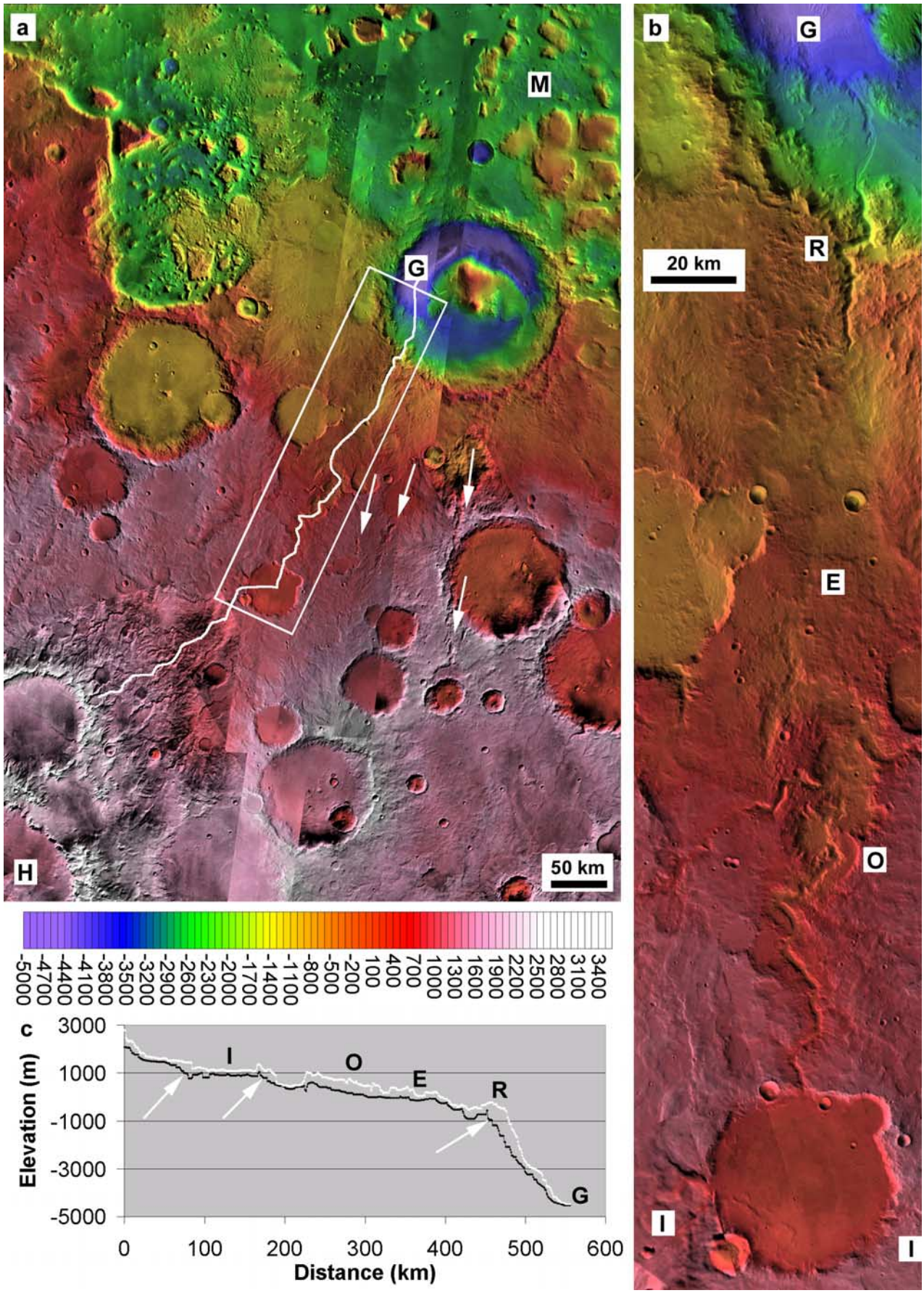
a
M
G
H
50 km
b
G
20 km
R
E
O
I
I
-5000
-4700
-4400
-4100
-3800
-3500
-3200
-2900
-2600
-2300
-2000
-1700
-1400
-1100
-800
-500
-200
100
400
700
1000
1300
1600
1900
2200
2500
2800
3100
3400
c
Elevation (m)
3000
1000
-1000
-3000
-5000
I
O
E
R
G
0
100
200
300
400
500
600
Distance (km)

**Figure 4**

pedestal craters), high past erosion rates, thermal properties, poor cohesion, and stratigraphic position with respect to craters and valley networks. The Gale ejecta blanket and secondary craters are exposed (possibly exhumed) to the south of the crater but are not observed to the north [*Greeley and Guest*, 1987], where they should occur if the crater were younger than the subdued cratered unit. Gale appears to be younger than most Noachian degraded craters, however. Few valley networks and gullies dissect the Gale crater rim [*Cabrol et al.*, 1999; *Edgett and Malin*, 2001; *Pelkey et al.*, 2004], and otherwise Gale retains all of the characteristics of a fresh impact crater as classified by *Craddock and Maxwell* [1993]: a rough ejecta blanket, raised rim, hummocky interior walls, secondary crater chains to the south, and presence of a (partially buried) central peak (Figures 3 and 4). This generally poor erosion suggests that Gale formed after the period of ubiquitous crater degradation, which terminated during the late Noachian as shown by fresh crater counts in the region of N(5) = 200–250 per $10^6$ km$^2$ [*Craddock and Maxwell*, 1990; *Irwin and Howard*, 2002]. The stratigraphic boundaries provided by the end of crater degradation and the development of Aeolis Mensae (Early Hesperian) tightly constrain the time of impact to near the Noachian/Hesperian boundary. This is consistent with the *Cabrol et al.* [1999] interpretation of the crater's age and *Malin and Edgett*'s [2000] interpretation that the interior layers were deposited during the Late Noachian Epoch. Emplacement ages cannot be uniquely established for deflated surfaces [*Malin and Edgett*, 2000], so the Amazonian age established by *Cabrol et al.* [1999] for the Gale floor materials is only a younger bound, particularly as it is based on only four craters >2 km in diameter.

[12] A valley network to the south of Gale supplied water to incise the crater's single entrance breach (Figure 4). Tributaries within this network begin on the rims of craters that overlie the larger Herschel crater rim (H in Figure 4a). In the middle of the drainage basin, flow was routed through a 46-km impact crater, which contains a concave floor deposit with ~200 m of relief, but we find no evidence of a delta or channel incision within the floor material (Figures 4b and 4c). The crater has a wide outlet valley (O in Figure 4b), which is buried by Gale ejecta along its lower reach (E in Figure 4b). This outlet valley contains a narrow inner valley, which also originates at the 46-km crater, indicating late-stage entrenchment of an older outlet valley by flows that were routed through the crater. The inner valley does not appear to be buried by Gale ejecta or modified by obvious Gale secondary craters, although the inner valley occurs entirely to the south of the Gale continuous ejecta, so a unique relationship between the age of the crater and that of the inner valley cannot be established. Another example of outlet entrenchment is discussed in section 2.3.

[13] A narrow, V-shaped valley segment is also incised into the Gale crater rim (R in Figure 4b). Overland flow from the south would be confined and directed over the Gale rim by two low ridges that trend perpendicular to the dichotomy boundary. A small enclosed basin occurs south of the crater rim between these low ridges (between R and E in Figure 4b), isolating this entrance breach valley from the contributing network upslope. Headward extension of the breach valley by entrenchment into the Gale rim would ultimately have connected the contributing network (O) to the entrance breach (R), but the breach was never incised deeply enough for this to occur.

[14] The Gale entrance breach and a second valley network that occurs on the inner wall of the crater both terminate on the crater floor at positive-relief deposits with frontal scarps (Figure 3; see detailed view in section 3). These deposits occur within separate enclosed basins, one north and one south of the central mound, respectively (Figure 3). Base level control of fluvial deposition or deflation from around an alluvial lag may be responsible for the frontal scarps. The southern deposit retains a more sharply defined scarp, above which the fan surface ends at approximately −3300 m, but the spillway in modern topography between the northern and southern sub-basins in Gale occurs at −3400 m. If these are deltas from separate paleolakes, then some aeolian modification of the interior mound must have occurred after fluvial activity ended permanently. However, confinement of one deposit in the higher southern basin suggests (but not uniquely) that the mound occurred generally in its present form when the fans or deltas were deposited. The mound is also somewhat dissected by fluvial channels, but the deposit terminal scarps are not, suggesting that erosion of the mound was contemporary with deposition of the alluvium.

[15] The northwestern side of the Gale floor at approximately −4500 m elevation is the lowest-lying surface in the crater's vicinity, so it would be a natural site for groundwater to emerge if a water table occurred above this elevation. The upper limit for the hypothetical paleolake surface is the −2450 m elevation of the intact northern crater rim, but the interior mound reaches an elevation of +488 m. This observation seems to rule out origin of the layered mound as a lacustrine deposit, as proposed by *Cabrol et al.* [1999], at least for the upper 3 km of its 5-km thickness [*Irwin et al.*, 2004b]. *Cabrol et al.* [1999] argued that an overflowing Elysium basin paleolake eroded the northern rim of the crater, but Mars Global Surveyor Mars Orbiter Laser Altimeter (MOLA) topography and Mars

**Figure 4.** A valley network that originates on the rims of craters overlying the northeastern side of Herschel crater (H) and terminates within Gale crater (G). The scene is centered at 8°S, 136°E. (a) Mosaic of Viking MDIM 2.1 and THEMIS daytime IR imaging (where available along the valley) colored with MOLA topography. The white line indicates the main stem of the valley network, the white box shows the location of Figure 4b, and the white arrows show radial chains of secondary craters from Gale. Aeolis Mensae (M) occurs to the north of the dichotomy boundary. (b) Enlargement of the lower reach of the Herschel-Gale network, north of a 46 km crosscut crater at the bottom of the frame. This crater has two inlet valleys (I) and one terraced outlet valley (O). Near Gale crater, ejecta (E) has buried and roughened the landscape, and a pristine, V-shaped entrance breach occurs in the Gale crater rim (R). The Gale interior is shown in Figure 3. (c) Longitudinal profile from MOLA shot data showing the Herschel-Gale valley thalweg and the highest adjacent surface within 3 km of the thalweg. White arrows indicate prominent knickpoints.

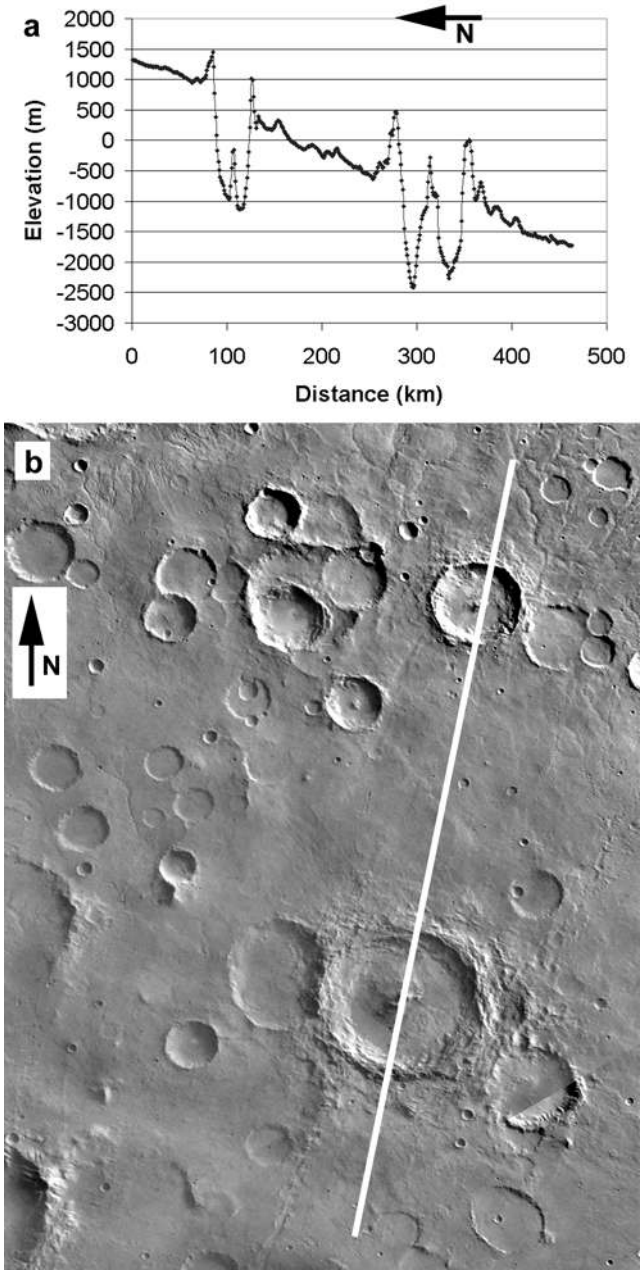


**Figure 5.** Topography of fresh impact craters emplaced on the northern interior slope of Hellas basin. (a) MOLA 60 pixel/degree gridded topography showing the tilt of the crater rims subparallel to the precursor slope. The crater cavities and central peaks are oriented vertically, rather than perpendicular to the slope, indicating that these craters were not tilted after formation. (b) Context image from the Viking MDIM 2.1, centered at 25.5°S, 87.5°E. The white line is the profile in Figure 5a.

Odyssey Thermal Emission Imaging System (THEMIS) imaging show that no distinct valley crosscuts the northern Gale rim, and furthermore no enclosed basin occurs between Elysium Mons and the highlands as proposed by *Scott and Chapman* [1995]. The present surface in Elysium Planitia is very level and at too low an elevation (−2650 to −2750 m) to overflow to Gale crater without flooding the entire northern lowlands to −2450 m; such a high sea level may be possible but has not been conclusively demonstrated [*Carr and Head*, 2003]. The low elevation of the crater rim along its northern margin does not require catastrophic erosion (it shows little evidence of erosion, catastrophic or otherwise), as it can be explained simply by an original tilt of the crater rim due to its location on the older dichotomy boundary slope [*Irwin et al.*, 2004b]. Fresh impact craters have rims that incline sub-parallel to the precursor slope, as shown in profiles across fresh impact craters in the Hellas basin (Figure 5). Gale crater may have contained one or two shallow paleolakes at low elevations (<−3300 m), but we find no compelling indication in the available data that lakes persisted for millions of years or more. If a long-lived paleolake did occur in Gale crater, it must have been supplied by groundwater, but observations are more consistent with a water table far below the present exterior surface, and perhaps even below the crater floor.

[16] In summary, the stratigraphy and erosional morphology of Gale crater suggest a mainly dry history with only minor fluvial erosion of the wall and central layered mound. The following sequence of events is suggested: (1) Late Noachian decline of highland valley network activity; (2) Gale impact; (3) burial of Gale crater and its ejecta by airfall materials; (4) erosion of Aeolis Mensae fretted/knobby terrain and deflation of the Gale crater fill to form the streamlined interior mound; and (5) a brief reactivation of highland valley networks that breached the Gale rim at its upslope low point, dissected the streamlined interior mound, eroded sparse gullies on the rugged crater interior wall, and deposited fans or deltas on the crater floor. At this site, we interpret a hiatus within an epoch of erosive valley network activity while the interior layers were deposited and partially deflated by wind. The other sites discussed herein may have experienced a similar hiatus, but without the stratigraphic marker offered by airfall materials, intermittent valley activity is more difficult to confirm or reject at those locations.

### 2.2. Pristine Exit Breach: Terraced Crater in Memnonia

[17] Aside from Gusev, Gale, and "Eberswalde" craters, a 48-km, unnamed crater in northwestern Terra Sirenum (14.6°S, 174.8°W) has probably received the most attention as a possible crater paleolake (Figure 6) [*Forsythe and Zimbelman*, 1995; *Cabrol and Grin*, 1999, 2001b; *Ori et al.*, 2000]. The crater is noteworthy for an undissected terrace that extends around the crater's interior and into its wide inlet valley (I in Figure 6). The terrace is broken only where a narrow, V-shaped outlet valley (O in Figure 6) cuts the northern crater rim, connecting the crater to a much wider, presumably older valley to the north (N in Figure 6b). Previous authors have interpreted the crater terrace as wave-cut or depositional, in either case controlled by a fairly stable lacustrine base level, but *Leverington and Maxwell* [2004] proposed an igneous origin for the terrace and the crater's inlet and outlet valleys. Using topographic tests, we show that volcanism is not a viable hypothesis for development of the crater terrace and valleys, so the only remaining alternative is a late-stage overflow by water of a previously enclosed basin.

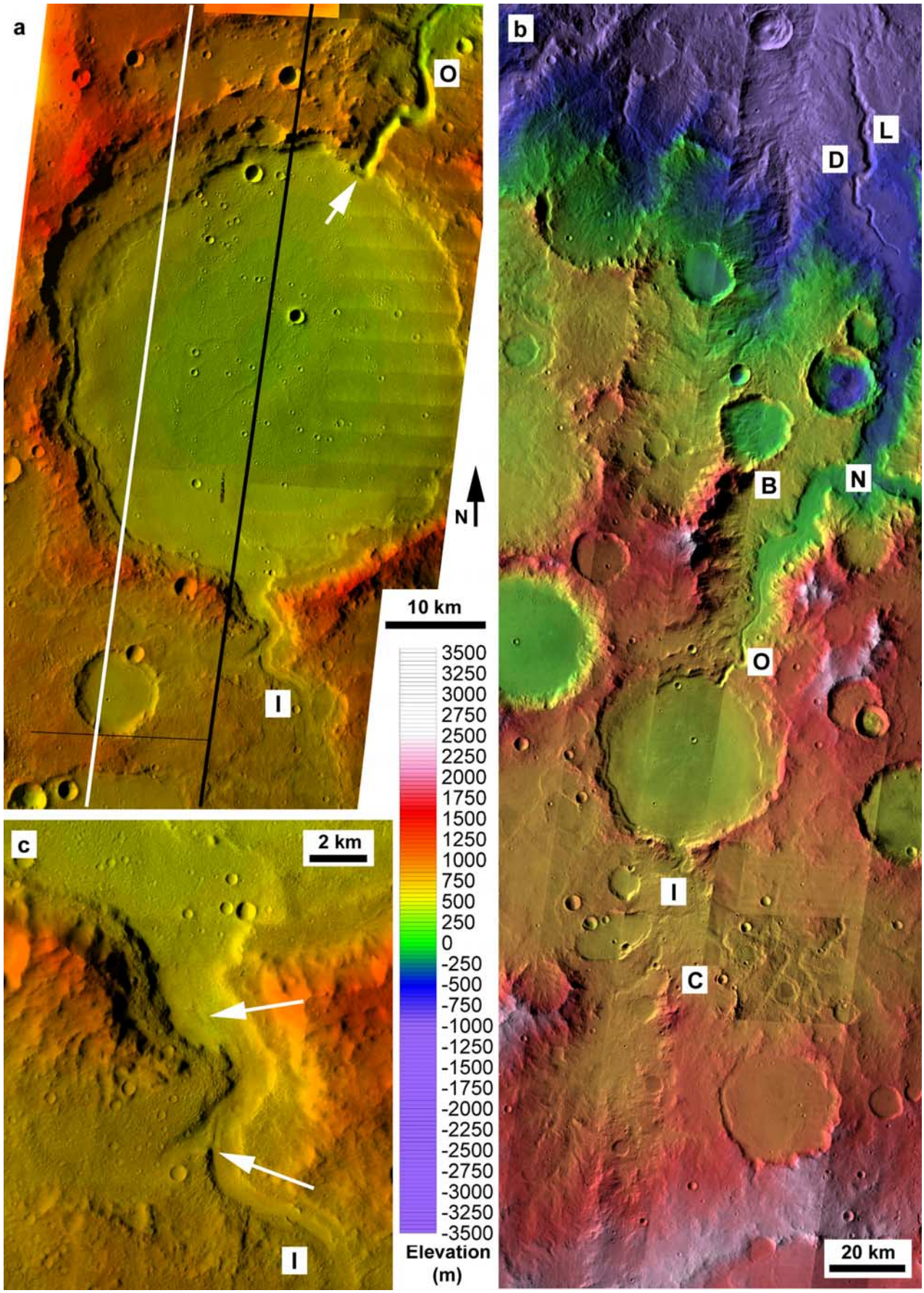
a
O
N
10 km
I
c
2 km
I
3500
3250
3000
2750
2500
2250
2000
1750
1500
1250
1000
750
500
250
0
-250
-500
-750
-1000
-1250
-1500
-1750
-2000
-2250
-2500
-2750
-3000
-3250
-3500
Elevation (m)
b
L
D
B
N
O
I
C
20 km

**Figure 6**

[18] The terraced crater occupies a topographic constriction between a contributing basin to the south (C in Figure 6b) and the wide northern valley. The floor of the wide northern valley is deeply incised near the terraced crater and also along a lower reach (L in Figure 6b) at the dichotomy boundary, which is a heavily cratered slope in this region (D in Figure 6b, Figure 7a). A lower-gradient middle reach of the northern valley does not contain a deeply incised inner valley. The contributing basin to the south of the terraced crater is ~300 km wide in the east-west direction and consists of several adjacent, highly degraded craters (Figure 7d). On the basis of their lower depth/diameter ratios and heavily degraded rims, the craters that formed the contributing basin appear older than the breached (but otherwise intact) terraced crater. The contributing basin floor occurs at >700 m elevation and is concordant with the 400–700 m elevation of a bench within the northern valley (B in Figure 6b); however, it is uncertain whether the northern valley predates or postdates the terraced crater. The bench is sloped inward and dissected, so it may represent an abandoned bajada or pediment surface. Below this bench, the outlet valley is approximately 7 km in width, which suggests either a prolonged period of base level stability or a period of aggradation following valley incision.

[19] The longitudinal profile of the inlet and outlet valleys is shown in Figure 7a. The outlet valley has a maximum depth of 400 m near its head. Given that this valley is only 1.9 km wide and has interior slopes averaging 23° at this location, its origin is more consistent with collapse or incision of a valley than with dimensions of either fluvial or volcanic bankfull channels. Small channels are locally evident on the inlet and northern valley floors (Figure 6c) and elsewhere in the region [*Irwin et al.*, 2005]. These channels are of appropriate width (150 m) to have been carved by runoff from the 23,000 $km^2$ area of the contributing basin. A channel-forming discharge of at least 800 $m^3/s$ and a contemporary runoff production rate of 0.3 cm/day are suggested by the inlet channel width, using the conservative method described by *Irwin et al.* [2005] and reviewed in section 5.

[20] *Forsythe and Zimbelman* [1995] argued for a fluvial or lacustrine origin for the crater terrace on the basis of three observations: (1) the terrace is developed within the crater and the inlet valley but not within the outlet valley (Figure 6a), which is consistent with base level control within the crater prior to the incision of the exit breach; (2) the inlet valley widens as it approaches the crater (Figure 6c), which is more consistent with prolonged fluvial erosion under base level control than with a volcanic rille; and (3) the terrace is relatively narrow along the outer margin of bends in the inlet valley, as expected for bank erosion by a meandering channel. Examination of Figure 6c does not compellingly support their third point, and these observations by themselves do not uniquely rule out a volcanic origin for the terrace, but the first two points are accurate and relevant. *Forsythe and Zimbelman* [1995] did not present conclusions on whether the terrace is wave-cut or depositional, but *Ori et al.* [2000] interpreted a wave-cut origin with little discussion of alternatives. We find this origin unlikely as the terrace has up to 50 meters of relief within its width of ~1–4 km, it does not appear wider along any preferred wind direction, and it is up to several times wider than wave-cut terraces on the Earth [see also *Leverington and Maxwell*, 2004] (wave energy is dissipated over distances <1 km [*Trenhaile*, 2001, 2002]). Furthermore, the occurrence of the similarly wide terrace within the inlet valley is not consistent with fetch-controlled erosion rates. The terrace is located within the upturned crater rim and it also crosses the rim at the inlet valley, both of which rule out a resistant outcrop as the cause along any part of its length [*Leverington and Maxwell*, 2004]. The inlet valley terrace likely resulted from dissection of the inlet valley floor as base level declined within the terraced crater. We find that the terrace width is greater in areas where the crater rim is higher (Figure 6a). These observations are consistent with origin of the terrace as a deposit of some kind and suggest more sediment production from areas where the crater rim has greater relief, as described by *Forsberg-Taylor et al.* [2004]. For a volcanic terrace, the relationship between terrace width and rim height would be only coincidental.

[21] Drainage within the contributing basin was partially directed toward local terminal basins (smaller degraded craters superposed on the wider contributing basin), and the area that drained directly to the terraced crater in the present valley configuration is primarily located to the south and southeast (Figure 7d). As with much of the Martian highlands, the densest drainage networks are located on relatively long, steep slopes at high elevations within the contributing basin, and the valleys originate near high crater rims or other divides (Figure 6b). The numerous branching valley networks in the contributing basin demonstrate that water flowed to the terraced crater (the terminal basin for these networks unless an overflowing paleolake occurred in the crater), as this basin-filling network planform is not observed in volcanic rilles. The grading of the inlet valley profile upstream of the terraced crater (Figure 7a) also implies throughflow of sediment to the crater.

[22] The inlet valley ends at an elevation of 570 m (our measurement differs somewhat from the 620 m value given by *Leverington and Maxwell* [2004]) where it enters the crater and becomes unconfined. The crater floor is locally graded flat to this elevation near the crater wall, outward of a central concave depression but below the terrace level (Figure 7c). The crater floor also occurs at 570 m at the

**Figure 6.** A terraced crater in Memnonia (14.6°S, 174.8°W), colored with MOLA topography. (a) THEMIS visible wavelength mosaic of the terraced crater, showing the inlet valley I and the outlet valley O. Note the greater width of the terrace in areas where the crater rim is higher. The white arrow indicates the head scarp of the outlet valley. The black and white lines are MOLA shot tracks 19273 and 12483, shown in Figures 7b and 7c, respectively. (b) Setting of the terraced crater, showing part of the contributing basin C, the wide northern valley N, the bench of the northern valley B, the top of the dichotomy boundary scarp D, and the lower reach of the outlet valley L. (c) Full-resolution (17 m/pixel) THEMIS VIS view of the incised lower reach and mouth of the inlet valley. White arrows indicate a ~150 m wide interior channel along the outer margin of one bend in the valley. Note the increase in valley width as the inlet valley approaches the crater.

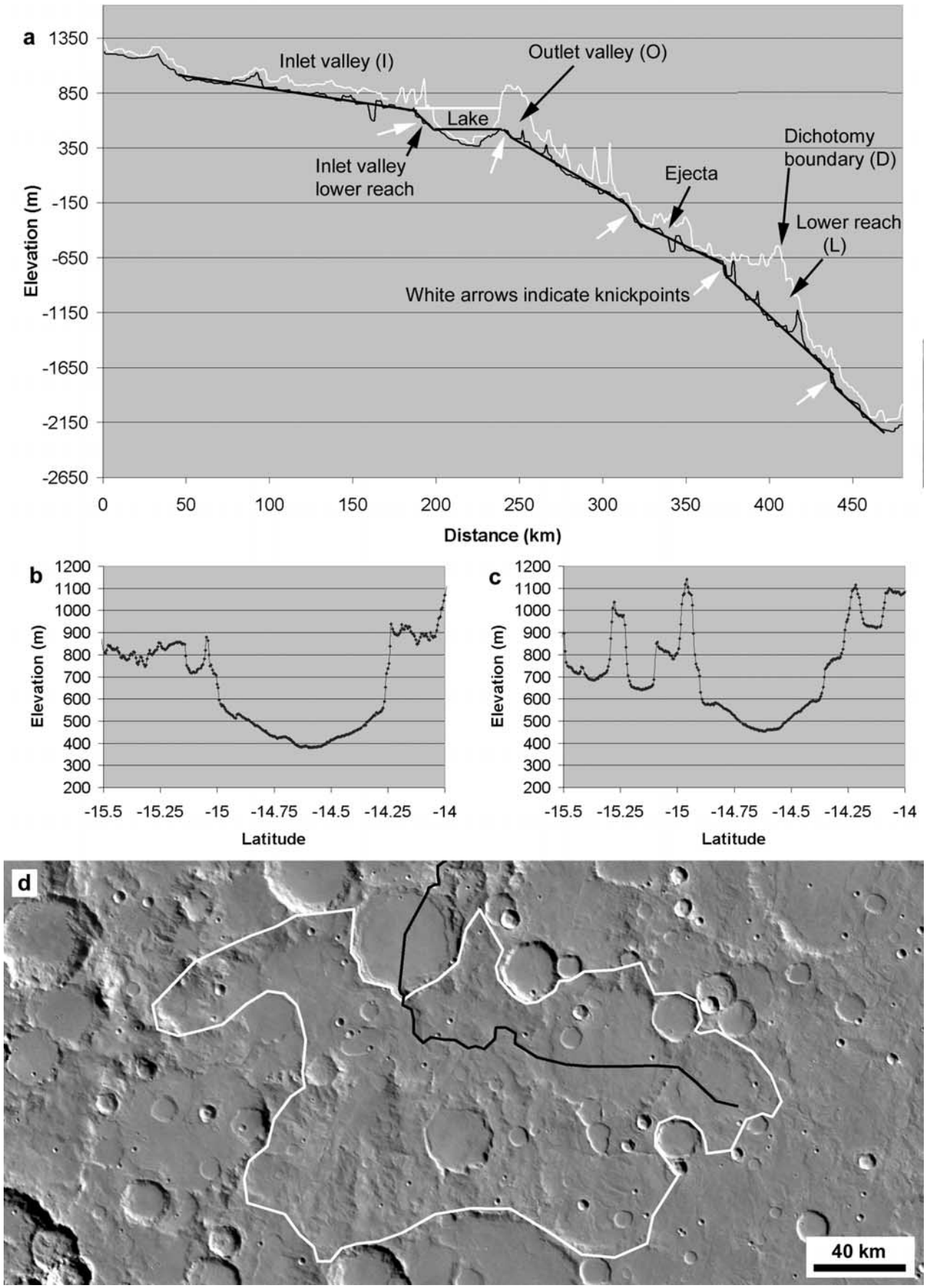
a
Inlet valley (I)
Outlet valley (O)
Lake
Inlet valley lower reach
Ejecta
Dichotomy boundary (D)
Lower reach (L)
White arrows indicate knickpoints
Elevation (m)
Distance (km)
b
Elevation (m)
Latitude
c
Elevation (m)
Latitude
d
40 km

**Figure 7**

outlet, all of which are consistent with a paleolake surface at 570 m. The low point on the crater floor occurs at 375 m, which leaves ~200 m of relief within a crater floor of 41 km diameter, or a mean gradient of 0.56°. This concentric slope is in line with fan gradients [*Craddock and Howard*, 2002], but recognized lava fills typically have relatively flat (e.g., the floor of Gusev crater) or outward-declining surfaces over large areas. A steep knickpoint (arrow in Figure 6a) is located at the head of the narrow outlet valley, where elevation drops rapidly from ~570 m to ~510 m. Without a paleolake in the terraced crater, there is no contributing aquifer above this elevation to provide water for sapping at this site. *Leverington and Maxwell* [2004] acknowledge the "blunt, amphitheater-like headwall" to the outlet valley but then state that "no local development of a nick point or plunge basin" occurs at this site. The headwall morphology is entirely consistent with origin as a spillway knickpoint. The outlet valley head has advanced ~500 m into the crater floor and >3 km headward from the crater rim (arrow in Figure 6a). This headward migration of a drainage divide is common to lake overflows that incise an outlet valley [*Irwin et al.*, 2004a].

[23] The crater terrace's inner margin maintains a level of ~720 m (Figures 7b and 7c) (this is an imprecise figure as MOLA shots have 170-m footprints and ~300-m spacing), which is also approximately the base level for the well graded upper reach of the inlet valley (measured at ~700 m, Figure 7a). This grading relationship indicates a base level control for the contributing networks that was well above the crater floor and coincident with the terrace elevation. *Leverington and Maxwell* [2004] state that "if the material that originally comprised the crater's inner wall contributed the terrace material, then it is not logical for the terrace to extend 10 km up the inlet valley." Their logical argument is flawed, however, as a 700-m lacustrine base level would affect both terrace deposition and inlet valley grading simultaneously, and the terrace material does not need to have a single provenance. The absence of a projecting delta at the 700-m level does not rule out a paleolake, as the entrenchment of the inlet valley's wide lower reach has broadly eroded the area where a delta might otherwise be found (Figure 6c). A bench at the ~570 m level in the crater (Figure 7c) may be composed of such a reworked deposit, the elevation of which was controlled by the base level of the exit breach. It is also relevant that the inlet valley has breached the crater rim to 4.5 km width [*Forsythe and Zimbelman*, 1995]. Fluvial erosion under base level control could produce a wide breach over time, but lava typically does not produce erosional channels that widen significantly in the downslope direction. No volcanic edifice occurs in the contributing basin, so the volcanic hypothesis for the entrance breach is without constructive support that would overcome these inconsistencies with basin morphology.

[24] Determining overflow elevations is complicated by the incision of the outlet valley, but one can measure the elevation of the top of the valley sidewalls for an estimate. The overflow elevation for the terraced crater could not be less than 850 m (the lowest elevation of the northern side of the crater rim, as measured in abundant raw MOLA shots) without invoking a precursor outlet valley, for which evidence is not preserved. This observation is significant in that the original crater rim was not the base level control for the terrace development and for the inlet valley above its knickpoint, both of which record a base level of 700–720 m. The overflow elevation is also relevant to *Leverington and Maxwell*'s [2004] proposal that the outlet valley formed by overflow of a lava lake, either by thermal erosion of the crater rim or as a constructional channel as lava resurfaced the area north of the crater. Such an overflow is impossible without flooding and completely burying degraded craters and valley networks in a considerable area of the contributing basin adjacent to the entrance breach, between the 700 and 850 m contours (Figure 8). Degraded craters and valley networks are still present in the area that would be flooded to this level (Figure 6b). For lava to exit the crater by breaching its rim, one must invoke the subsurface lava flow they propose as an alternative; however, the outlet valley is sinuous and therefore does not independently suggest structural control of subsurface flow. The valley course is entirely consistent with surface flow over pre-valley topography, and the outlet valley originates at the low point on the crater rim. The width of the outlet valley decreases with distance from the crater rim, which is similar to lunar rilles [*Leverington and Maxwell*, 2004], but as the valley walls are very near the angle of repose, the narrowing is also the logical result of the declining valley depth with distance from the elevated crater rim. The overflowing lava lake concept also does not explain the concave form of the crater floor that occurs in place of more typical caldera topography.

[25] A further challenge for the volcanic hypothesis lies in the longitudinal profile of the outlet valley (including its lower reach), which consists of several straight segments separated by knickpoints. The lower reach is incised up to 700 m below the northern valley surface, and its longitudinal gradient is steeper than is the outlet valley thalweg near the terraced crater (Figure 7a). This incision requires a

**Figure 7.** Topography of the terraced crater and its through-flowing valleys. (a) Longitudinal profile determined from MOLA shot data. The thin dark line represents MOLA shots along the valley thalweg, whereas the thin white line is the highest elevation within 2.5 km from the thalweg, here used to represent the exterior surface. The thicker dark line is an interpretation of valley segments and knickpoints (white arrows) indicated by the topography. The thick white line is the elevation of the inner margin of the crater terrace, well below the spillway of the crater. Note the grading of the inlet valley to the terrace level, the occurrence of a remnant basin in the terraced crater below the outlet level, the deep entrenchment of the outlet valley's upper and lower reaches in areas of steep slope, and knickpoints. (b) Concavity of the crater floor in the center-crossing MOLA shot track 19273. (c) A second lower terrace is locally evident on the western side of the crater floor in MOLA shot track 12483. Also note the 50 m of relief within the northwest side of the upper terrace. Locations of these profiles are shown in Figure 6a. (d) Drainage divide for the contributing basin. The dark line is part of the longitudinal profile shown in Figure 7a. North of the crater, the longitudinal profile follows the outlet valley thalweg.

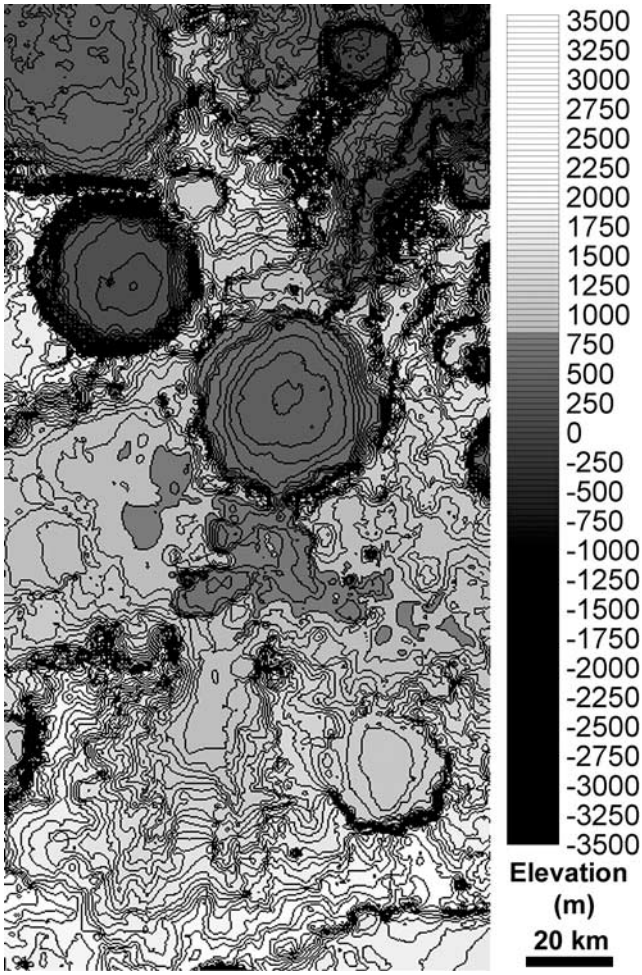


**Figure 8.** MOLA contour map, 128 pixels/degree, 50 m contour interval, of the terraced crater and vicinity. The darker shade within and south of the crater shows the area that would be flooded during an overflow of the terraced crater at its 850 m spill point. A considerable area south of the terraced crater would be inundated with lava if an overflowing lava lake formed the outlet valley, but degraded impact craters and valley networks are still exposed below 850 m elevation in this area (Figures 6b and 7d). The concave floor of the crater is evident, which is also not suggestive of basaltic infilling. The area is bounded by 174°W, 176°W, 13°S, and 15°S.

recovery of erosive power ~130 km down-valley from the crater rim. As the depth of these narrow valleys increases with precursor slope, we find general agreement with erosion rates that are proportional to stream power, but to recover its erosive power a lava flow would need very high effusion rates, given the progressive loss of heat, increase in viscosity, and the eventual transition from turbulent to laminar flow with distance from the source. High effusion rates are not suggested by constructional landforms in the terraced crater or its cratered contributing basin. As the two inner valleys are sharply incised into a crater rim and the dichotomy boundary scarp, respectively, erosion of substrate materials is required to create them rather than development of a volcanic channel through levee aggradation (the two alternatives suggested by *Leverington and Maxwell* [2004]). These observations are all consistent with a fluvial origin for this system.

[26] Other features invoked by *Leverington and Maxwell* [2004] as indications of volcanism, such as peripheral moats and ridges on the terraced crater floor, are likely structural features that are not uniquely associated with any one geologic material. The lobate margin in their Figure 3b is an erosional scarp that bounds the lower reach of the inlet valley and is not a flow front. Given the energy requirements to heat and melt country rock, and the loss of heat to the surrounding rock and the atmosphere, the thermal surplus of lava is inadequate to thermally erode more than small, localized areas, so volcanism is primarily a resurfacing process. Large constructive lava channels are possible, but here the necessary work is erosive against a precursor crater rim.

[27] *Leverington and Maxwell* [2004] state that "Maintenance of lake level at roughly the same elevation over a sufficiently long period to form the terrace, only to subsequently fall as a result of substantial outlet incision, cannot be accounted for without invoking unlikely scenarios involving catastrophic flood events that are inconsistent with the nature of the central crater and the inlet basin." The occurrence of other pristine, entrenched lower reaches of many valley networks on Mars refutes this argument. Such late-stage entrenchment was common [*Baker and Partridge*, 1986] and may reflect widespread higher (but not catastrophic) runoff production over a short interval at the end of fluvial activity [*Howard and Moore*, 2004; *Howard et al.*, 2004; *Howard et al.*, 2005]. Alternatively, integration of previously enclosed basins upslope can rapidly change the total water budget, resulting in basin filling and entrenchment of lower reaches. In the paleolake Bonneville basin, U.S.A., a transgression of the lake (leading up to its catastrophic overflow) initiated when a lava flow diverted the Bear River into the Bonneville basin. The Bear River now provides 43% of the present inflow to Great Salt Lake [*Malde*, 1968]. In this contributing basin on Mars, any of several crosscut impact craters could have produced the same effect locally, although basin overflow upslope would be necessary to explain the downslope overflow, so basin capture does not necessarily simplify the history. It is important to note that the occurrence of this crater terrace, which has 50 m of relief within its width, does not require perfect maintenance of lake level, and the terrace may also have been undercut at the 570-m level. It is also possible that a narrow precursor outlet valley, incised to the 700-m level, controlled the lake level for a time, only to be subsequently downcut and enlarged by an increase in discharge. An ice cover may have slowed water loss from the lake, insulating this or other Martian lakes from rapid changes in level. The volume of the terraced crater is ~400 km$^3$ between the 850 m and 570 m levels, and the combined volumes of the outlet valley and the lower reach are ~20 km$^3$, assuming V-shaped valleys with sidewalls at 23°. A water-to-sediment volume ratio of ~20:1 would be available to carve the valleys from a paleolake overflow without recharge, or a much larger water volume may have been available from contributing basin runoff. The convex-up profile of the crater terrace is not dissected, nor are the sidewalls of the outlet valley, which rules out significant

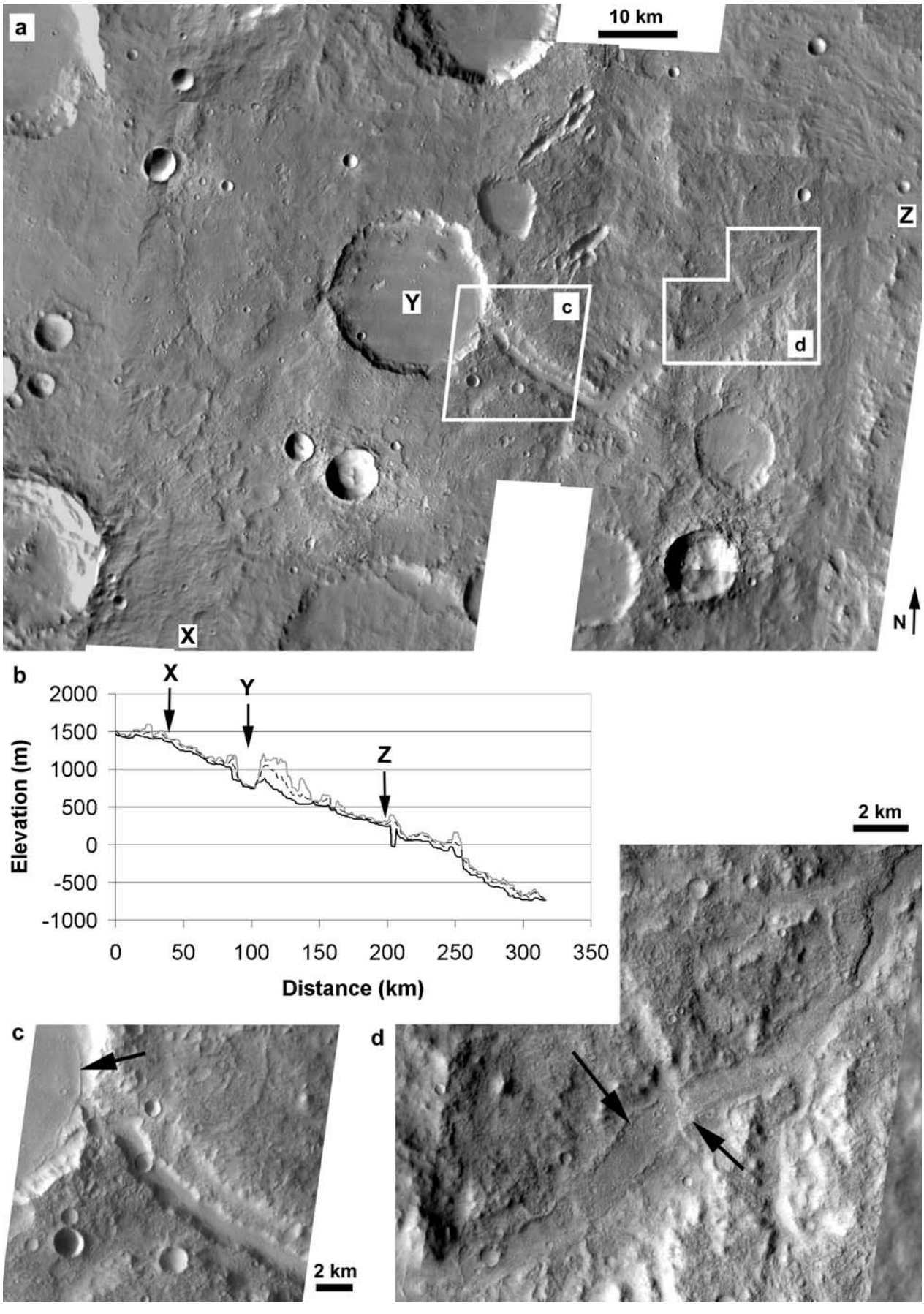
a
10 km
X
Y
Z
c
d
N
b
Elevation (m)
2000
1500
1000
500
0
-500
-1000
0
50
100
150
200
250
300
350
Distance (km)
2 km
c
d
2 km

**Figure 9**

precipitation runoff after the exit breach and terrace formed [*Leverington and Maxwell*, 2004].

[28] On the basis of the evidence available, the original conclusions of *Forsythe and Zimbelman* [1995] are supported relative to the occurrence of a paleolake in this basin; however, it remains uncertain to what extent this may have been an evaporite basin as they suggested. Fluvial activity was the last major erosive event to occur in the contributing drainage basin and is most likely responsible for the outlet valley entrenchment. No observation uniquely confirms the hypothesis that the crater floor deposit, terrace, or any related valleys had a volcanic origin, and we conclude from topographic data that a lava lake overflow did not form the outlet valleys. However, some minor volcanic resurfacing of the terraced crater floor or other localized basin surfaces cannot be ruled out with existing data.

### 2.3. Entrenchment of a Precursor Outlet Valley: Unnamed Crater in Terra Sirenum

[29] *Cabrol and Grin* [1999] interpreted (without specific discussion) another paleolake within a 21-km crater in Terra Sirenum (18.3°S, 169.2°W, Figure 9). Like the terraced crater in Memnonia and the 46-km crater along the Herschel-Gale valley network, this crater has an inlet valley with a steep lower reach, a wide outlet valley, and an entrenched inner valley within the outlet. The inlet valley or channel has been partly buried by fresh impact crater ejecta near X in Figures 9a and 9b. Above its knickpoint the inlet valley is graded to ~1040 m, which is a possible paleolake highstand, as this is also the elevation of the outlet valley terrace at the exit breach. The steep lower reach of the inlet valley terminates at the ~900 m margin of the crater floor (meters to a few tens of meters of uncertainty attend the MOLA measurements on steep surfaces). This is also the elevation of the outlet valley head, which is consistent with a low water stage. The basin's low point occurs at 744 m on the eastern half of the crater floor. No knickpoint or headwall is evident at the outlet valley head (Figure 9c). This crater has no continuous interior terrace, but some terrace development is evident along the southern wall of the crater. The crater rim has been extensively eroded, so this terrace segment may be a resistant outcrop of upturned rock, but aqueous depositional processes are also possible. The terrace has an irregular surface but no lobate projections that would indicate a mass-wasting origin. On the northern side of the crater floor several knobs occur, which may be coherent blocks shed from the crater wall or remnants of a previously more extensive deposit on the crater floor. It is possible, but uncertain, that the long, curvilinear, sharp-crested ridge on the crater floor (black arrow in Figure 9c) developed by shore processes during the terminal stage of the paleolake, when it may have been covered by ice. Whether formed by shoreline or structural processes, the ridge postdates the crater's overflow, as it blocks the outlet valley. The outlet valley terrace walls are poorly dissected, so a relatively brief, late epoch of entrenchment is more reasonable than prolonged incision of the outlet's inner valley by precipitation runoff.

[30] As with previous examples, the wide terrace of the outlet valley records a geomorphic surface (Figure 9c), and delivery of water to the outlet terrace surface requires a paleolake in the crater with a level at 1040 m, coincident with the inlet valley grading. Entrenchment of the outlet valley and a decline in lake level to ~900 m would have left a residual paleolake on the undissected crater floor. The most reasonable cause for this suite of landforms is a late-stage increase in stream power applied to the terrace surface, but not necessarily a single catastrophic flood. Down-valley, the inner valley or channel is not deeply incised but is defined instead by marginal ridges or levees (black arrows in Figure 9d). If a flow occupied the entire 700–800 m width between the low bounding ridges, downslope from the exit breach, then a discharge of 4900–5800 $m^3/s$ would be indicated [*Irwin et al.*, 2005], or a runoff production rate of ~2.3 cm/day from the 19,000 $km^2$ contributing area. Runoff production rates this high are possible, but the putative channel is wider than has been observed in valley networks without an enclosed basin at their head [*Irwin et al.*, 2005]. Drawdown of a paleolake within the crater would be a more reasonable water source, which could have been initiated and augmented by a much smaller runoff volume from upslope.

[31] The terraces in the wide outlet valley and the lack of a delta complex are anomalous, with respect to terrestrial paleolakes, but we can speculate on circumstances that might be reasonable for Mars. In an environment where Martian impact craters filled with water only during discrete episodes or brief epochs of flow, the lake levels would be highly variable, and delta development would be inhibited by slope failures and/or density currents at high water stages and by fluvial or aeolian reworking at low stages. An ephemeral flow regime would not provide the necessary stability to accumulate a delta, despite the occurrence of a high outlet. With respect to the wide outlet valleys, such a climate would also support the relative stability of the outlet valley level. Coarse material could be derived from the valley sidewalls during low- or no-flow conditions and reworked during the infrequent overflows, which may be near the threshold for gravel transport. Thus the outlet would, through widening, provide the material necessary

**Figure 9.** A breached 25-km crater in Terra Sirenum (18.3°S, 169.2°W). (a) Context mosaic of THEMIS visible wavelength imaging. The flow direction was from X to Y to Z, and the white boxes indicate the insets in Figures 9c and 9d. The valley's longitudinal profile is modified by fresh crater ejecta near X. (b) Longitudinal profile of the valley from MOLA shot data. The black line is the thalweg, the gray line is the exterior surface, and the dashed line shows the elevation below which 75% of the MOLA shots are located (given to approximate the terrace elevation within the outlet valley). Note the grading of the inlet valley to the outlet terrace level and the remnant basin below the level of the entrenched outlet. (c) The terraced outlet valley of this crater, enlarged from Figure 9a. The black arrow indicates a ridge at the outer edge of the crater floor. (d) Raised ridges indicated by black arrows bound a possible inner channel downslope from the breached crater. The channel is only slightly wider than the entrenched outlet valley floor, suggesting that the same discharge of water formed both features.

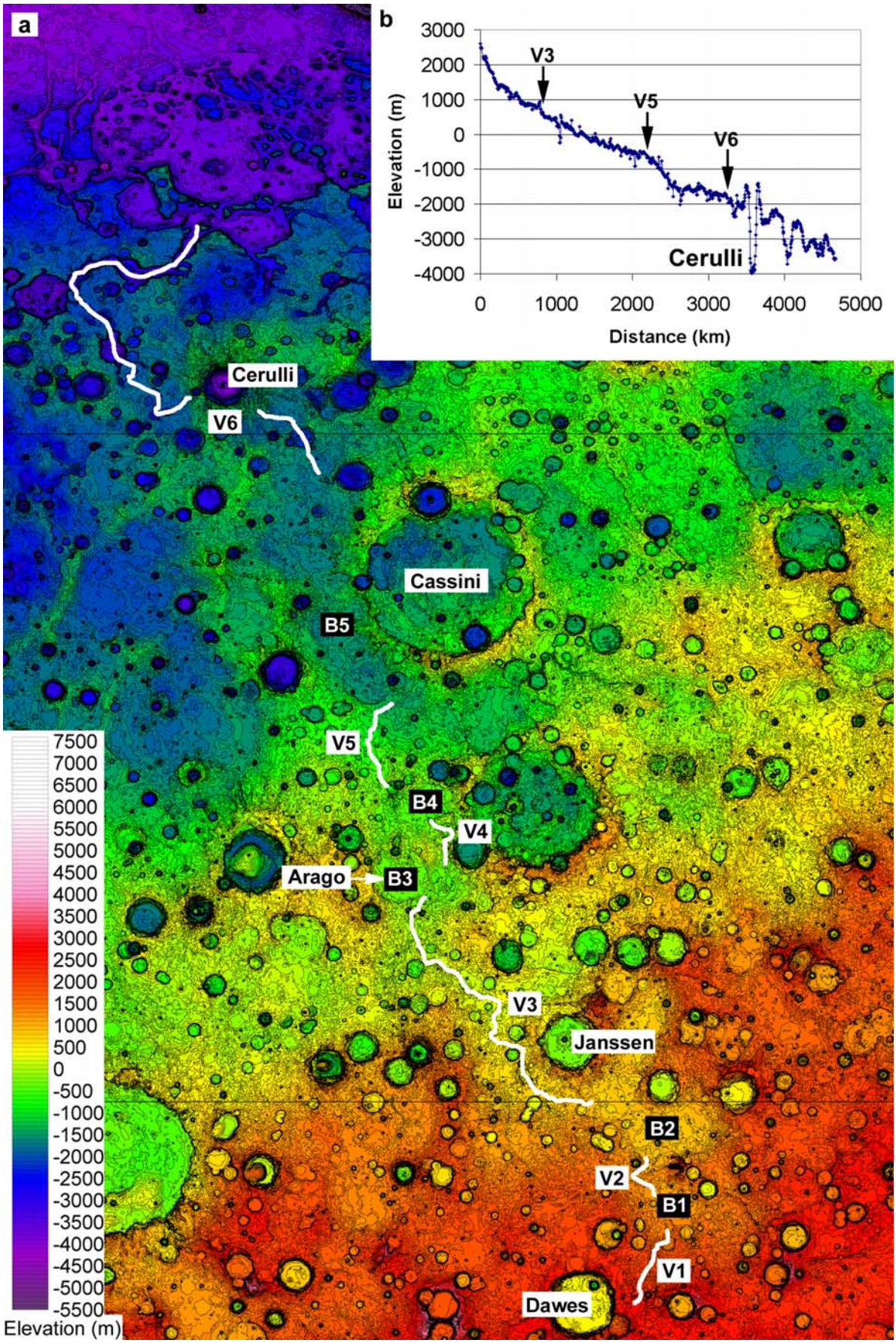
a
b
3000
2000
1000
0
-1000
-2000
-3000
-4000
Elevation (m)
V3
V5
V6
Cerulli
0
1000
2000
3000
4000
5000
Distance (km)
Cerulli
V6
Cassini
B5
V5
B4
V4
Arago
B3
V3
Janssen
B2
V2
B1
V1
Dawes
7500
7000
6500
6000
5500
5000
4500
4000
3500
3000
2500
2000
1500
1000
500
0
-500
-1000
-1500
-2000
-2500
-3000
-3500
-4000
-4500
-5000
-5500
Elevation (m)

**Figure 10**

to stabilize its topographic level. Finally, entrenchment of the pristine inner valley in the outlet would probably require a late-stage increase in discharge.

### 2.4. Extension of a Multibasin Valley Network: Naktong/Scamander/Mamers Valles

[32] While investigating the source areas for pristine valley segments, we identified a series of interconnected basins in Arabia Terra, which collectively form one of the longest valley networks on Mars, with a total length of 4700 km (Figure 10). This valley network offers several examples of late-stage basin overflow and pristine valley entrenchment, and we can use the variable tributary development along its length to isolate the source regions for most of the discharge. Deep entrenchment along this valley network is localized within the through-flowing stem valley (Figure 11a), which was supplied by relatively dense but shallow valleys on the contributing slopes to the south (Figure 11c).

[33] The Naktong/Scamander/Mamers network begins in a set of drainage basins around and including V1/V2 in Figure 10, which lie immediately to the north and east of Dawes crater (9°S, 38°E, 180 km diameter). These valley networks debouched northeast of Dawes to a broad intercrater plain, which incorporates two very shallow basins (B1 and B2 in Figure 10). The B2 plain appears to have formed upslope from a low ridge of ejecta from the 160-km Janssen crater (2.5°N, 37.5°E). This ejecta divide, the spill point of the lower basin B2, is also the head of Naktong Vallis (V3 in Figure 10). Naktong Vallis is joined by several major tributaries (Figure 11c; see Figure 2a for detail) along its 950 km course to the B3 basin, which consists of the 150-km Arago crater and another overlapping, highly degraded crater (Figure 11b). A second valley segment (V4) exits the B3 basin and connects it with another basin (B4) located 130 km to the north. The B4 basin occurs at the head of Scamander Vallis (V5), which is noteworthy in that the valley has only six tributaries over its 240 km length, and most of these are not well graded to the stem valley floor (Figure 11a). Scamander Vallis and another major valley network from the east (Indus Vallis) debouch to a large arcuate basin (B5) west of and adjacent to Cassini crater. This B5 basin occurs at the head of Mamers Vallis (V6), the large sinuous fretted valley that *McGill* [2000] and *Carr* [2001] interpreted as having been initially carved by fluvial processes, but with a later overprint of ice-facilitated mass wasting [see also *Squyres*, 1978; *Mangold*, 2003]. This mass wasting and resulting debris apron development account for the irregular longitudinal profile of the modern Mamers Vallis floor (V6 in Figure 10b) [*Lanz et al.*, 2000]. The head of Mamers Vallis occurs on the B5 basin floor, southeast of the 115-km fresh crater Cerulli, which overlies the upper reach of Mamers Vallis. The heads of these valley segments occur within enclosed basins, so ponding is likely required to incise the narrow outlets. Following this outlet incision, some of the basin floors may have contained through-flowing shallow channels that do not stand out in the available imaging and topography, possibly due to subsequent autocompaction or other modification of the basin floors. The pristine, steep-walled morphology of northern reaches with little tributary development (Figures 11a and 11b) suggest a relatively brief period of throughflow in the combined network. Long-lived precipitation would have developed more sidewall gullies and/or tributaries than are observed, and slower development by sapping from a regionally distributed aquifer would have a similar effect.

[34] A detailed interpretation of this large valley network would require a separate study, as it covers 4700 km from its source area to its mouth in Deuteronilus Mensae, across diverse geologic terrains. The declining tributary development and relatively pristine morphology at higher latitudes in this network suggest that the northern reaches (V4–V6) developed later than Naktong Vallis (V3) and its tributaries, and/or that runoff production declined with elevation and distance northward from the main source area in the highlands. For the present purpose, the late incision of pristine, narrow valleys to integrate previously enclosed, highly degraded basins demonstrates that late-stage, relatively voluminous flows from the equatorial highlands downcut to base levels in the fretted terrain. *McGill* [2000] dated Mamers Vallis to the Early Hesperian Epoch, which is consistent with our interpretation of terminal valley network activity in Aeolis Mensae (section 4).

## 3. Development of Deltas During Late-Stage Valley Entrenchment

[35] Well-preserved depositional landforms provide important clues to paleoclimate history, but the development of a substantial delta requires several specific conditions. (1) Deep water over a long period of time or high sediment delivery rates are required for thick deltas to accumulate. (2) A relatively stable water level and shoreline are necessary to limit reworking of deposits at low water stages and lateral or radial migration of the river mouth within the basin, leaving no prominent lobe in any one location [e.g., *Blair and McPherson*, 1994]. Closed lakes (which have no surface outlet) are often subject to large volume and level changes [*Cohen*, 2003, pp. 166–167]. (3) The influx of sediments to the delta must exceed the capacity of processes redistributing the sediment within the basin, including after the lake receded [*Gilbert*, 1890]. Sand-bed channel fill and overbank delta deposits are particularly susceptible to

**Figure 10.** The Naktong Vallis/Scamander Vallis/Mamers Vallis drainage basin, one of the longest valley networks on Mars. (a) MOLA 64 pixel/degree topography of the drainage basin, cylindrical projection, bounded by 11°S, 49.1°N, 12.2°E, and 52.1°E. For scale, Cassini crater is 430 km in diameter. Basins and connecting valleys (white lines) are numbered sequentially in the downstream direction. V3 is Naktong Vallis, V5 is Scamander Vallis, and V6 is Mamers Vallis. (b) Longitudinal profile connecting the labeled valleys and the intervening basins, derived from MOLA shot data. The incised heads of Naktong, Scamander, and Mamers Valles are labeled. Note the concave grading of the valley up to the Scamander Vallis head, the steep reach along the deeply incised, V-shaped Scamander Vallis, and the Cerulli impact and modification of the longitudinal profile by debris apron development along Mamers Vallis.

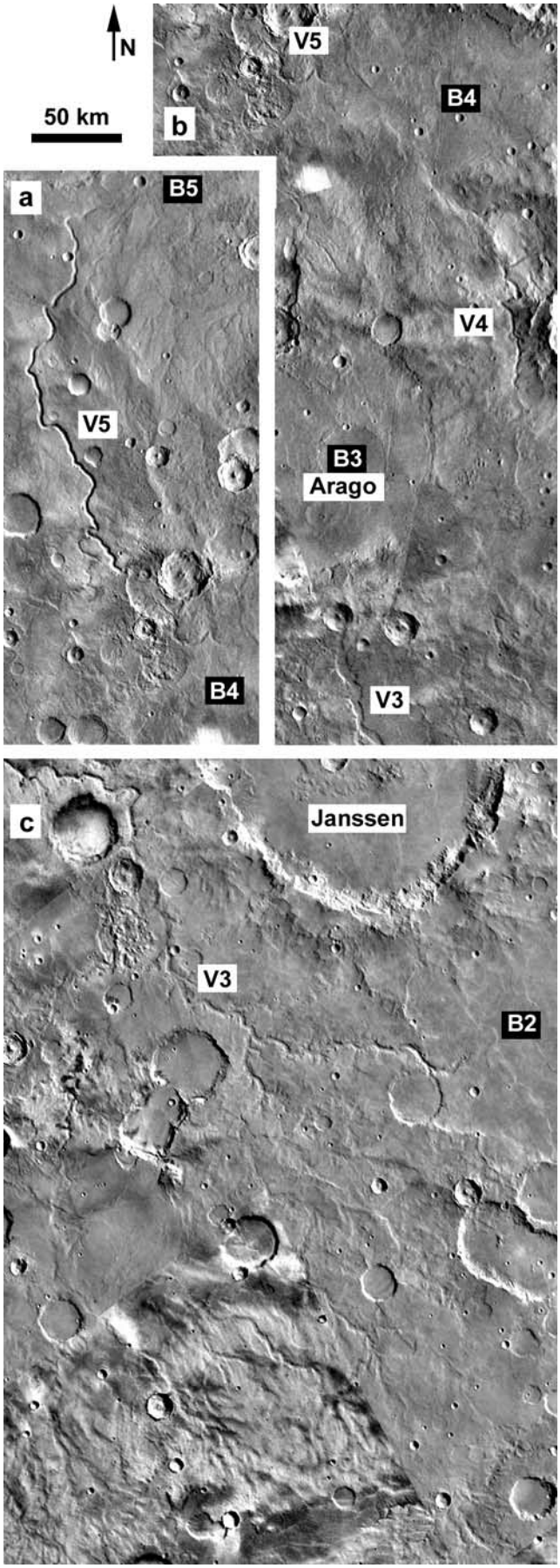


fluvial reworking at low lake levels (Figure 12). In deep, steep-walled basins, such as volcanic or impact craters, deltas may not develop because slope failures can effectively transport sediment away from the water surface and deposit it as underwater fans [*Cohen*, 2003, p. 210]. For these three reasons, delta development is inhibited in deep, steep-walled lakes and shallow ephemeral lakes [*Cohen*, 2003, p. 181], but the occurrence of a delta requires that conditions of longevity, stability, and ineffective redistribution processes were met at some point. Deltas exhibit a steep peripheral scarp at their outer margin, a genetic distinction that contrasts with the slightly concave longitudinal profile of alluvial fans. Examples of the latter on Mars are described by *Williams et al.* [2004] and *Moore and Howard* [2005].

[36] For a delta to be entirely removed by aeolian processes after a lake disappears, it must be composed of grains $<\sim$4 mm in diameter, as wind cannot transport larger particles [*Greeley and Iversen*, 1985, p. 55]. Alternatively, some weathering process must be available after deposition to reduce the grain diameter of the alluvial lag. An entirely fine-grained composition would require very low peak discharges, particularly in immature fluvial systems. Where inflowing channels breached Martian craters but high-relief deltas are not observed, either deep lakes did not occur (playas remain a possibility), or a combination of aqueous and aeolian weathering and/or transport processes (but likely not wind alone) reworked the deltas at low-water stages. Absence of deltas requires that one or more of the three conditions above were not met, or a period of ephemeral fluvial activity occurred after a paleolake disappeared. Conversely, preservation of deltas would require a (geologically) rapid and complete decline in the environmental conditions that supported the lake. The presence or absence of deltas is thus highly relevant to the paleoclimate, the nature of climate change, and basin hydrology.

[37] In a survey using new high-resolution imaging, we relocated and examined (where possible) the putative deltas that have been reported in prior Mars literature, and we identified several previously unreported deposits (Table 1). *Cabrol and Grin* [1999] listed most of the deltas that have been reported to date; however, clear scarp-fronted deposits do not occur in most of the craters where they reported deltas. In several cases, we may simply be making a more conservative interpretation of features that they observed in Viking imaging, but *Malin and Edgett* [2003] targeted

**Figure 11.** Detail of the Naktong Vallis/Scamander Vallis/Mamers Vallis drainage basin from the Viking MDIM 2.1. Basins and valley reaches are labeled as in Figure 10. (a) Scamander Vallis (V5), the steepest reach in the network, and the reach with the most prominent V-shape and least tributary development (centered at 15.6°N, 29.3°E). The V5 reach may have formed later than headward reaches, during an overflow of the B4 basin. (b) The V4 valley connecting the B3 and B4 basins (centered at 11.1°N, 30.8°E). (c) The Naktong Vallis (V3) headwater region, where tributaries are denser (centered at 0.6°S, 37.2°E; see detail in Figure 2a). We infer from the increasing tributary density with elevation that most of the runoff from this drainage basin originated in the elevated headwater regions to the south.

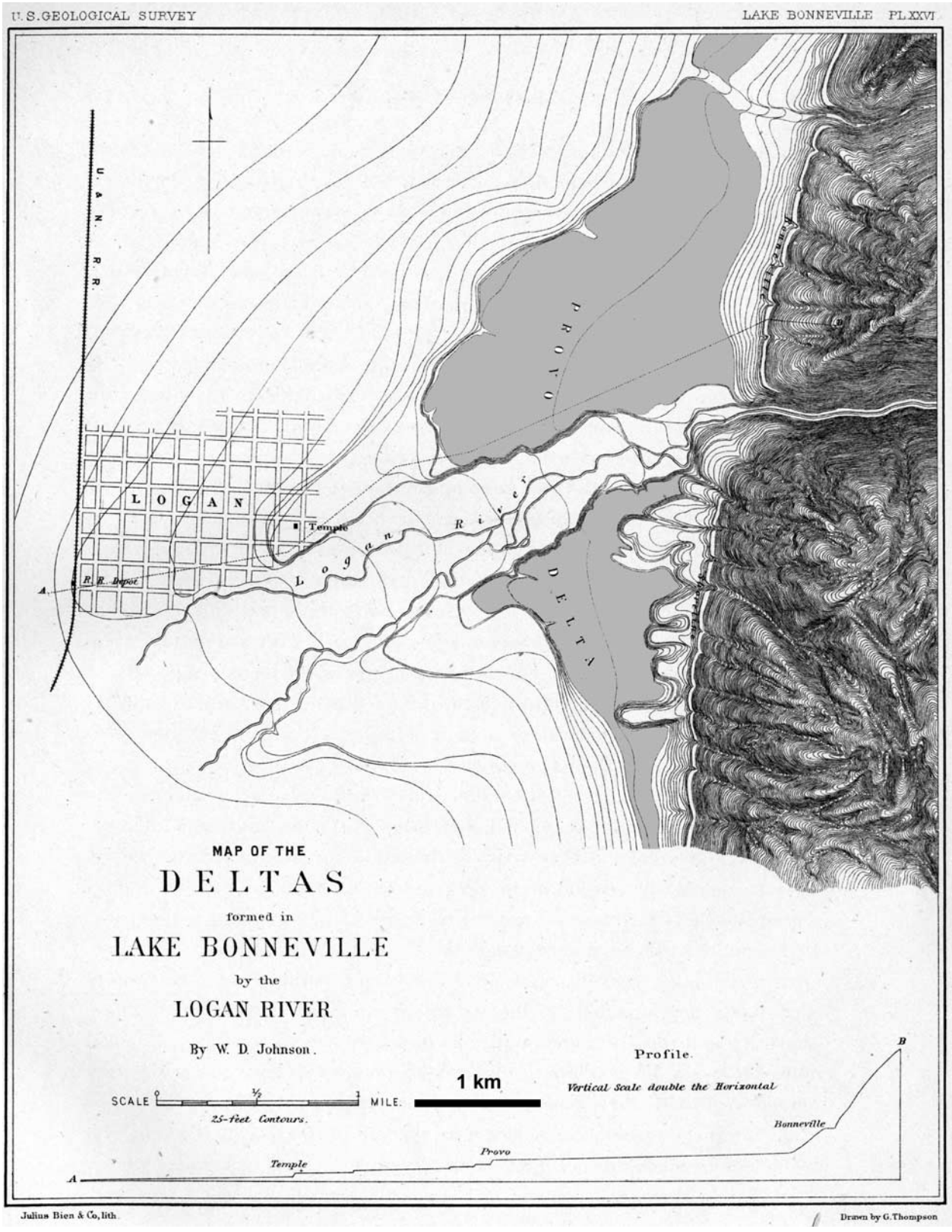


**Figure 12.** The paleodelta of the Logan River at the Provo shoreline of paleolake Bonneville, adapted from Plate 26 of *Gilbert* [1890] (41.74°N, 111.79°W). The delta topset of the Provo stage is indicated in gray shading. Above (eastward) of the Provo topset is the small remnant of an older delta, which formed at the higher Bonneville stage and was largely reworked at the Provo stage. Base level decline in Lake Bonneville subsequent to about 14.2 kyr ago resulted in rapid entrenchment of the Logan River into the delta surface. Any highstand deposits within the contributing valley were also largely removed.

**Table 1.** Positive-Relief Deposits With Frontal Scarps at Valley Mouths

| Crater Name, Diameter | Type[a] | Location, Quadrangle | Reference Image (Figure Number) | Width × Length, km | First Reported by |
|---|---|---|---|---|---|
| 1. Unnamed, 10 km | N | 30.9°N, 12.3°E Ismenius Lacus | Viking 206S07 (Figure 13a) | 1.7 × 1.5 | *Grant and Schultz* [1993] |
| 2. Unnamed, 62 km | N | 33.9°N, 17.5°E Ismenius Lacus | THEMIS V11845005 (Figure 13b) | 9.0 × 5.3 | *Cabrol and Grin* [1999], #19 |
| 3. Unnamed, 33 km | N | 34.3°N, 18.1°E Ismenius Lacus | THEMIS V11221010 (Figure 13c) | 4.2 × 5.9 | *Cabrol and Grin* [1999], #20 |
| 4. Unnamed, 42 km | N | 12°N, 52.7°W Lunae Palus | THEMIS V12359011 (Figure 13e) | 4.7 × 1.9 | *Cabrol and Grin* [1999], #39 |
| 5. Unnamed, 48 km | N, F | 6.25°S, 149.47°W Memnonia | Viking 456S07 THEMIS I09442025 (Figure 13f) | 4.5 × 2.3 | *Ori et al.* [2000] |
| 6. Unnamed, 39 km | N, S | 15.65°S, 155.2°W Memnonia | Viking 444S30 (Figure 18a) | 3.3 × 1.8 | *Ori et al.* [2000] |
| 7. Unnamed, 72 km | N, S | 8.6°S, 159.27°W Memnonia | THEMIS V10579001 (Figure 18b, 18d) | 11.8 × 7.9 | *Ori et al.* [2000] |
| 8. Unnamed, 33 km | N, S | 7.96°S, 146.58°W Memnonia | THEMIS I01379001 (Figure 18c) | 6.5 × 4.7 | *Cabrol and Grin* [2001b] |
| 9, 10. Gale crater, 160 km | N N | 5.37°S, 137°E 5.8°S, 137.3°E Aeolis | THEMIS V04852001 THEMIS V07436001 (Figure 13d) | 13.8 × 10.5 16.5 × 10.7 | *Cabrol and Grin* [2001b] |
| 11. Unnamed, 38 km | N, T | 5.13°N, 58.6°W Lunae Palus | THEMIS V05844020 (Figure 13g) | 7.1 × 3.7 | *Cabrol and Grin* [2001b] |
| 12. Holden crater, 150 km | N | 26.8°S, 34.5°W Margaritifer Sinus | THEMIS V03210003 (Figure 16d) | 15.5 × 24.5 | *Grant and Parker* [2002] |
| 13. Unnamed, 13 km | N | 28.0°N, 26.7°E Arabia | Viking 214A15 (Figure 15b) | 2.7 × 5.2 | *McGill* [2002] |
| 14. Unnamed, 80 km | N | 28.1°N, 27.2°E Arabia | THEMIS V11620010 (Figure 15b) | 6.6 × 14.0 | *McGill* [2002] |
| 15. Unnamed, 57 km | N | 29.5°N, 25.7°E Arabia | THEMIS V04880003 (Figure 15c) | 5.5 × 13.8 | *McGill* [2002] |
| 16. Unnamed, in fretted valley | S, F | 35.5°N, 26.3°E Ismenius Lacus | THEMIS V12581003 (Figure 15a) | 10.8 × 4.4 | *McGill* [2002] |
| 17. "Eberswalde" crater, 64 km | D | 23.8°S, 33.7°W Margaritifer Sinus | MOC2-543a mosaic (Figure 16c) | 13 × 11 | *Malin and Edgett* [2003], *Moore et al.* [2003] |
| 18. Holden crater, 150 km | D | 27.0°S, 34.45°W Margaritifer Sinus | THEMIS V03210003 (Figures 16d, 16e) | 10.4 × 10.2 | *Pondrelli et al.* [2005] |
| 19. Unnamed, 89 km | N | 27.9°S, 83.1°E Iapygia | THEMIS V08012002 (Figure 14a) | 14.3 × 10.6 | *Howard and Moore* [2004] |
| 20. Aeolis Mensae | N | 3.65°S, 132.7°E Mare Tyrrhenum | THEMIS I01256009 (Figure 14c) | 17.1 × 7.3 | *Irwin et al.* [2004b] |
| 21. Aeolis Mensae | N, F | 5.15°S, 132.85°E Mare Tyrrhenum | THEMIS I01256009 (Figure 14d) | 17.2 × 10.0 | *Irwin et al.* [2004b] |
| 22. Aeolis Mensae | D | 6.75°S, 151.1°E Aeolis | THEMIS I05588001 (Figure 17a) | 35.7 × 21.5 | *Williams and Edgett* [2005] |
| 23, 24. Unnamed, 56 km | D D | 18.4°N, 77.6°E Syrtis Major | THEMIS I00921002 (Figure 17b) | 9.2 × 5.4 8.6 × 7.9 | *Fassett and Head* [2005] |
| 25. Unnamed, 23 km | N | 39.2°S, 256.6°E Thaumasia | THEMIS I01265004 (Figure 15e) | 7.6 × 6.0 | *Mangold and Ansan* [2005] |
| 26. Nepenthes Mensae | N | 2.1°N, 121.6°E Amenthes | THEMIS V09832020 (Figure 14b) | 8.0 × 4.6 | this paper |
| 27. Unnamed, Parana, 25 km | D, T, F | 23.5°S, 12.1°W Margaritifer Sinus | THEMIS V09538003 (Figures 16a, 16b) | 5.3 × 3.2 | this paper |
| 28. Unnamed, 10 km | D | 19.08°S, 6.35°W, Margaritifer Sinus | THEMIS V08115003 (Figure 17c) | 3.9 × 3.3 | this paper |
| 29–33. Unnamed, 68 km | N, S<br>N, S<br>N<br>N<br>N | 27.9°N, 11.6°E Arabia | THEMIS V11658008 (Figure 15d) | 3.2 × 4.1<br>3.6 × 2.7<br>4.8 × 4.3<br>4.3 × 4.0<br>4.8 × 4.6 | this paper |

[a]N, no distributary network evident (scarp-fronted deposit); D, distributary network evident (scarp-fronted fan); S, stepped deposit; T, frontal scarp is entrenched; F, fan-head trench evident.

~200 Mars Orbiter Camera (MOC) images of 80 sites where deltas had been reported or where valley networks terminate in a crater, also finding "no discernable expression of deposition" in most cases.

[38] *Cabrol and Grin* [1999] published a list of 179 highland impact craters in which they found one or more of the following features: deltas, terraces, layered deposits, sedimentary deposits, evaporites, shorelines, and interior mounds. In order to focus on deltas related to valley networks, a number of critical issues with the data set must first be corrected (Table 2). *Cabrol and Grin* [1999] indicated whether craters were breached by contributing

**Table 2.** Evaluation of the *Cabrol and Grin* [1999] Paleolake Data Set

| Critical Observation | Applicable Basin Numbers in Paleolake List[a] | Comments |
|---|---|---|
| Crater is listed twice. | (56, 59) (113, 114) (178, 179) | Two numbers in parentheses represent the same crater. |
| Two craters overlap, with an eroded rim between them so that floor deposits are contiguous. These form a single basin. | (5, 8) (7, 10) (83, 86) (90, 93) (130, 131) (135, 136) (142, 144) (159, 160) | For (83, 86), the Mangala outflow breached the dividing rim. Craters (135, 136) are Gusev and an interior buried crater Thyra. |
| Crater is listed as modified by valley networks but was modified most recently by an outflow channel. | 35, 46, 77, 83, 90, 93, 106, 111, 118 | The Mangala outflow breached all but 35 and 46. Maja Vallis breached 35, and a spur of Tiu Vallis breached 46. Eight other listed craters were breached by Ma'adim Vallis, which is listed as a valley network but may have formed quickly during a paleolake overflow. |
| Crater is listed as modified by an outflow channel but was modified only by, or most recently by, valley networks. | 36, 39, 45, 48, 75, 80, 82, 84, 85, 88, 89, 92, 99, 105, 108, 110, 116, 129, 174 | 15 other craters not listed here were interpreted as modified by outflow channels only because they are located on the dichotomy boundary and contiguous with lowland plains. |
| Delta is not observed in crater where it was reported (only includes craters modified by valley networks). | 15, 28, 38, 41, 42, 44, 47, (56, 59), 57, 60, 61, 63, 65, 67, 68, 69, 70, 71, 73, 75, 78, 81, 82, 88, 95, 97, 98, 102, 103, 104, 105, 108, 113, 114, 115, 122, 126, 127, 133, 136, 137, 146, 149, 151, 154, 155, 162, 165, 167, 169 | This is a widespread discrepancy between this data set and our observations. We only report on sites where THEMIS imaging is available. See discussion in text. |
| Delta is observed in crater but was reported absent. | 48, 89 | Delta in 48 noted by *Cabrol and Grin* [2001b]. Delta in 89 noted by *Ori et al.* [2000]. See Table 1.2. |
| THEMIS imaging is not available for examination. | 40, 84, 128, 150 | No deltas are evident in the Viking MDIM 2.1. |
| Evaporites were not identified. | 95, 133, 134, 150 | Evaporites cannot be confirmed in any of the four basins where they were reported. |
| Interior layered deposit was invoked as evidence for a paleolake, but the deposit stands higher than basin rim. | 41, 85 | 41 is Henry crater, 85 is Gale crater (see section 2.1). |
| Crater may have a gullied rim, but it did not receive drainage from exterior valley networks. | 4, 5, 8, 12, 13, 17, 18, 28, 29, 38, 40, 41, 44, 47, 52, 55, 58, 87, 91, 94, 96, 97, 99, 102, 103, 105, 120, 121, 129, 150, 153, 166, 173, 174 | A water source from exterior valley networks was one of the criteria for identification of a paleolake. |

[a]Table 1 of *Cabrol and Grin* [1999].

valley networks or outflow channels, which is important as an outflow channel may have filled a basin only once, whereas repeated smaller flows in valley networks would support a different depositional environment that contains more information pertaining to paleoclimate. Nine craters were reported to have been modified by valley networks, but they were actually breached by named outflow channels (we remain consistent with *Cabrol and Grin* [1999] in classifying Ma'adim Vallis as a valley network). Conversely, 19 craters grouped with the outflow channels are located far from the circum-Tharsis and Chryse regions, and these craters were in fact breached by highland valley networks. *Cabrol and Grin* [1999] may have believed that other small outflows occurred, beyond those that are generally recognized, but this possibility is not substantiated in their paper. Fifteen craters that are located along the dichotomy boundary, with rim breaches opening to the lowlands, were thought to have been supplied with water from the outflow channels. As many of these highland/lowland boundary craters are located on the opposite side of the planet from the Chryse region, this interpretation presumes a lowland ocean between these breached craters and their source outflow channels, and neither the occurrence nor the high-stand level of such an ocean have been uniquely demonstrated to date [*Malin and Edgett*, 1999; *Carr and Head*, 2003; *Tanaka et al.*, 2003].

[39] Taking this reclassification of water sources into account, *Cabrol and Grin* [1999] reported 65 deltas within equatorial highland (30°S–45°N) impact craters that are breached by valley networks. Of these, 50 show no indication of a delta at THEMIS visible or infrared resolutions (18 and 100 m/pixel respectively). In these 50 cases the contributing valley simply terminates at the crater floor, and no elevated deposit is evident. Three of the 179 craters in their paleolake database have valleys that exit the crater, but no valleys enter these craters that could have provided sediment for a delta. For example, *Cabrol and Grin* [2001b] reported a delta within Aram Chaos (see their Figure 6), but more recent topographic data shows that the channel actually exits the crater at this site as a tributary to

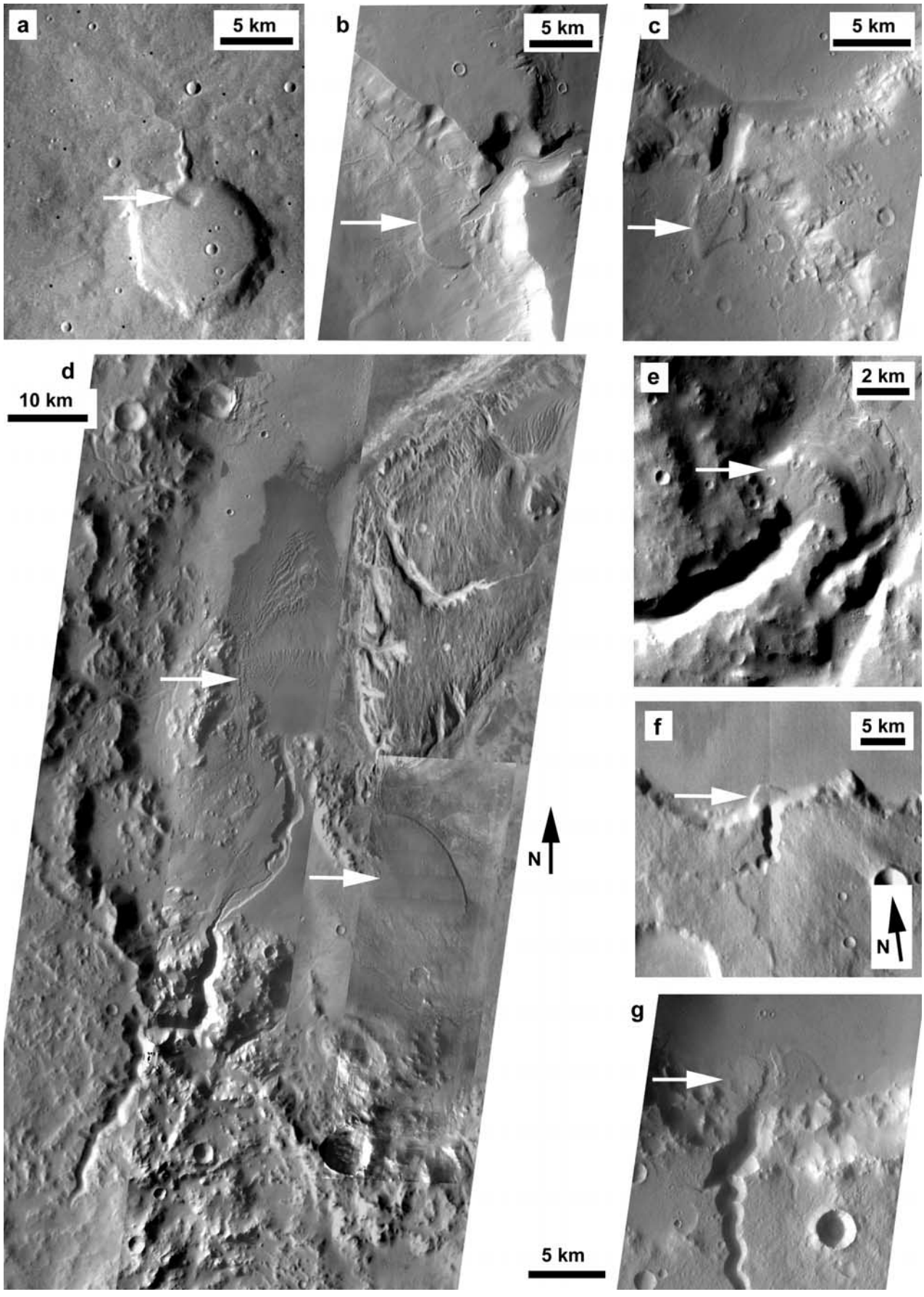


**Figure 13**

Ares Vallis. Of the remaining 15 craters reported to have deltas, four had inadequate THEMIS coverage to examine the entire site, but we were unable to relocate these reported deltas using the Viking Mars Digital Image Mosaic (MDIM) 2.1, which is derived from the same data set used by Cabrol and Grin. Six other craters have promontories or knobs at the inlet valley mouth that may be eroded fluvial deposits (2, 36, 43, 109, 135, and 143). Of these 65 craters, only three contain features that resemble unmodified deltas (19, 20, 39), and *Ori et al.* [2000] and *Cabrol and Grin* [2001b] later identified two deltas in craters that were reported to have no deltas in the *Cabrol and Grin* [1999] paper (48 and 89).

[40] Despite the large number of craters and other basins with contributing valley networks, only 33 positive-relief deposits are known at valley mouths. In Table 1 and Figures 13–18 we include all known highstanding valley-terminal deposits that have a frontal scarp, including fans with stepped surfaces. To remain genetically neutral, these deposits are hereafter termed ''scarp-fronted deposits'' where no distributary channel network is evident, ''scarp-fronted fans'' with distributary channels, and ''stepped deposits'' where a cone-shaped deposit is segmented by multiple scarps. Eight deposits are recognized for the first time in this paper, and more such discoveries may be made over time. We do not include the alluvial fans identified by *Williams et al.* [2004] and *Moore and Howard* [2005], as the toes of these fans are concordant with the crater floors and therefore do not suggest base level control by a lake.

[41] *Cabrol and Grin* [1999, 2001b] suggested that widespread crater paleolakes occurred during the Hesperian and possibly extended into the Amazonian Period. The low superimposed crater populations on these small basins yield large age errors that often cover two or more epochs, however, and the use of >2 km fresh craters yields younger stratigraphic ages on the *Tanaka* [1986] scheme than does the >5 km crater population on the same highland surface [*Irwin et al.*, 2004a]. Ages of the last paleolakes are therefore imprecisely known.

### 3.1. Scarp-Fronted Deposits

[42] Scarp-fronted deposits have a rounded, triangular, or projecting planform, and 18 of the 33 deposits now recognized (Figures 13–15) show little to no evidence of channelization, fan-head trenching, scarp dissection, or segmentation that would indicate a variable erosional and depositional history. Erosive fluid flows did not dissect the deposits after the base level declined in the terminal basin (contrast the Lake Bonneville delta in Figure 12 with the Martian deposits in Figures 13a–13f). The break in slope above the terminal scarp is often abrupt, as occurs in a *Gilbert* [1890] type delta at the topset/foreset boundary near the lake surface, but at least one example exhibits a more rounded, convex-up outer margin (#12 in Table 1, center of Figure 16d). The Uzboi Vallis terminal deposit in Holden crater has large ripples on its surface, which suggested to *Grant and Parker* [2002] that the deposit formed underwater.

[43] The observed scarp-fronted deposits occur at the ends of valleys that have V-shaped cross-sections and little or no tributary development along their entrenched lower reaches. Whether fed by spring discharge or precipitation runoff, these valleys and their terminal deposits represent late-stage flows, and the preservation of the deposits without later dissection suggests that the flows ended rather suddenly. Among the 33 positive-relief deposits listed in Table 1, 14 were derived from branching valley networks that commonly have wide undissected areas between tributaries. Eleven contributing valleys have basins above the valley head (shallow enclosures outside the crater and bounded in part by the crater rim or ejecta topography), such that the incised valley is disconnected from contributing slopes. Five deposits were sourced from incised gullies within a single crater rim, and three short valleys have indeterminate source areas due to poor image resolution. These characteristics are all consistent with a geologically brief period of source valley entrenchment and deposition.

### 3.2. Scarp-Fronted Fans

[44] *Malin and Edgett* [2003] and *Moore et al.* [2003] described the most compelling fluvial deposit on Mars, a scarp-fronted distributary fan in the 65-km ''Holden Northeast'' or ''Eberswalde'' crater in Margaritifer Sinus (#17 in Table 1, Figure 16c). Wind has differentially eroded the fan surface, and the channel fills have resisted deflation more effectively than have the overbank deposits, so inverted channels occur on the fan similar to those found in Oman [*Maizels*, 1990] and some other terrestrial deserts. These raised channels show a clear record of aggradation and avulsion in the form of scroll bars and meander cutoffs, but weathering and deflation of the coarser channel fill has been inadequate to remove this texture since the time of deposition, presumably over 3.6 billion years ago. Furthermore, the surface of the delta was not incised with decline of the lake level, again suggesting that the flows and surface weathering declined very abruptly. The two deltas identified by *Fassett and Head* [2005] (#23 and 24 in Table 1, Figure 17b) have a broadly similar morphology.

[45] Another distributary fan or delta occurs in a 25-km crater along the southern margin of Parana basin in Margaritifer Sinus (#27 in Table 1, Figures 16a and 16b). In this case, the fan exhibits a major entrenched channel and smaller distributary channels also in negative relief. The

**Figure 13.** Scarp-fronted deposits (white arrows) with no evident distributary channels in highland impact craters. These deposits all occur at the ends of pristine, entrenched lower reaches of valley networks, and only one of the deposits has an entrenched surface (Figure 13g; compare to Figure 12). (a) Scarp-fronted deposit in Arabia Terra. (b and c) Deposits in a chain of two breached craters that form a tributary to Mamers Vallis. Figure 13b is located immediately to the southwest and downslope of Figure 13c. (d) Southwestern side of Gale crater, showing the entrance breach from the south, two scarp-fronted deposits on the crater floor, sparsely dissected crater interior and central mound, and rugged crater rim. (e) Deposit in Lunae Palus with minimal dissection of the surface but no distributary network. (f) Deposit in Memnonia. (g) Deposit in Lunae Palus with entrenched surface. Reference image numbers, locations, and literature references are given in Table 1. North is at the top of all frames except Figure 13f, as indicated.

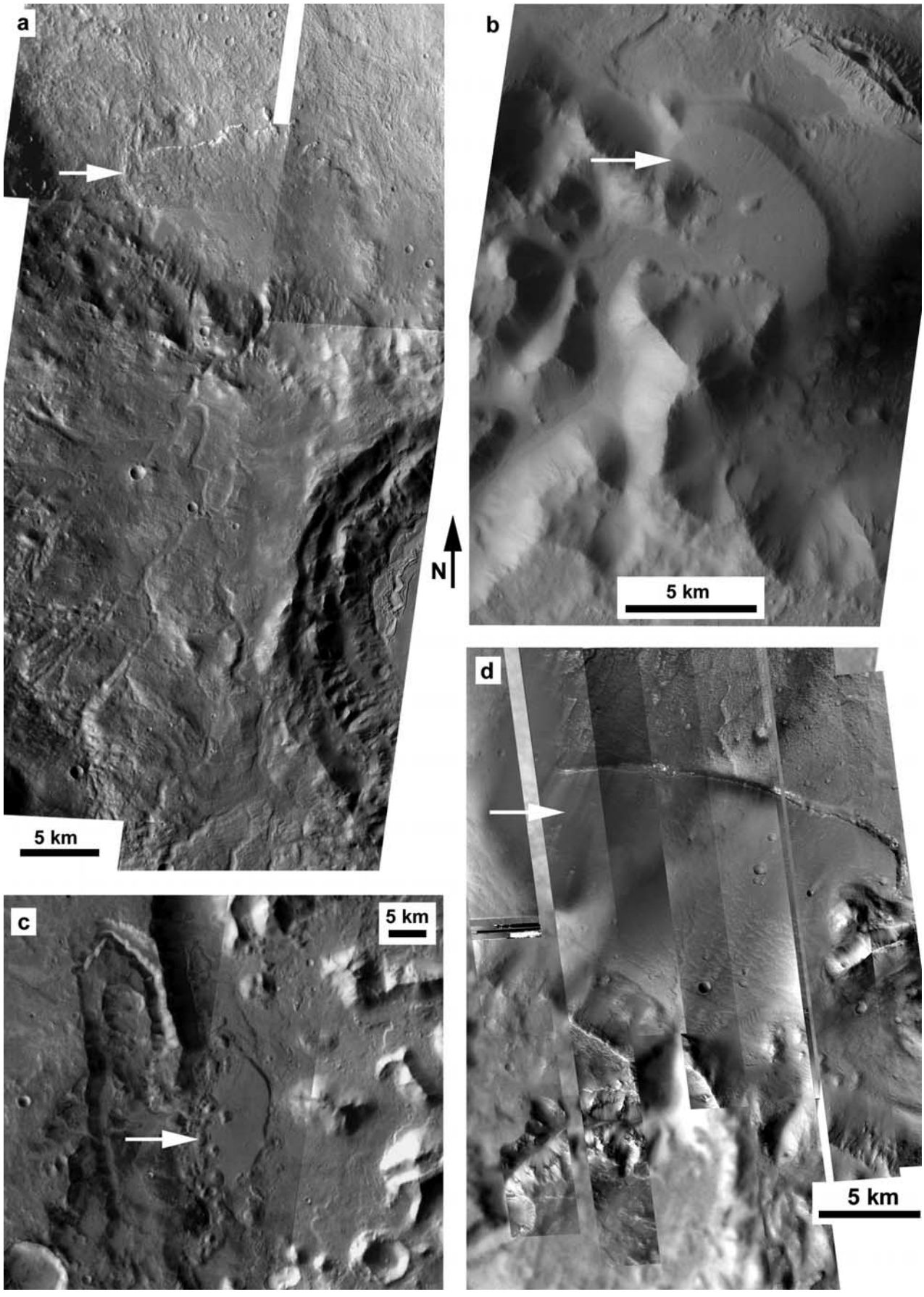


**Figure 14**

large channel was likely incised as the crater's exit breach formed and the lake level declined below its original spill point at approximately −775 m. This distributary fan also occurs at the distal end of a pristine, V-shaped, entrenched lower reach of a valley network (Figure 16b). These observations suggest that the fan was deposited as the contributing valley incised, followed by exit breaching and entrenchment of the fan surface. As with the "Eberswalde" fan and other scarp-fronted deposits, only one discrete epoch of persistent flow is required, and only limited fluvial activity could have occurred after the fan was emplaced. A similar situation is evident in another crater in Margaritifer Sinus (#28 in Table 1, Figure 17c), where a crater contains both an incised outlet and a deposit with a somewhat entrenched surface.

[46] Holden crater contains a concentration of large alluvial fans, which are more common in that region than elsewhere on Mars [*Moore and Howard*, 2005]. Among these is a scarp-fronted, segmented fan with a distributary network preserved on its surface in positive relief (#18 in Table 1, Figures 16d and 16e) [*Pondrelli et al.*, 2005]. The terminal scarp may be primary, resulting from deposition into standing water, or secondary as a result of scarp backwasting. We tested these alternatives using the eight MOLA shot tracks that cross the terminal scarp. Six of these indicate a toe (the fan surface at the head of the terminal scarp) elevation of −2160 ± 5 m, but the scarp heads at ~100 m higher elevations along the two westernmost shot crossings. This disparity suggests that either (1) backwasting created the terminal scarp along at least part of the fan, but debris from this process is not evident, or (2) the fan may have developed in stages, prograding into a receding paleolake in Holden crater. Smaller scarp-fronted fans terminate at higher elevations to the east and west of and adjacent to the primary structure, perhaps supporting the latter alternative. The terminal Uzboi Vallis deposit in Holden crater that was interpreted as subaqueous by *Grant and Parker* [2002] (#12 in Table 1, center of Figure 16d) occurs entirely below −2160 m, except where it has been modified adjacent to a crosscutting graben. This observation is consistent with standing water in Holden crater below that topographic contour.

### 3.3. Stepped Deposits

[47] At least six examples of stepped deposits have been identified within Martian basins [*Ori et al.*, 2000; *Cabrol and Grin*, 2001b; *Weitz et al.*, 2004], three of which are shown in Figure 18 (#6, 7, and 8 in Table 1). These deposits are punctuated by two or more scarps that are continuous around the cone-shaped surfaces, and there is little to no dissection of the deposit surfaces or the heads of the scarps. Alternative processes that might explain this unusual morphology are (1) an increase in base level during deposition, creating successive stacked fan-deltas at increasing elevations with time; (2) erosion of the deposit by shore processes at variable levels subsequent to emplacement; or (3) emplacement of the deposit segments as a sequence of debris flows of decreasing extent, wherein the peripheral scarps would be a primary feature. The first alternative would require a single-event origin for the stepped deposits and a rising lake level during deposition to explain the lack of dissection of the scarps (the event would probably have to be somewhat episodic in depositional intensity and/or water level rise to develop a stepped surface). Furthermore the sediment yields would need to decline (a possible effect of declining gradient in the contributing stream), or the rate of change in lake level would need to increase as lake level rose, so that the older underlying deposit segments were not overridden and buried. The scarps appear only on the deposit surfaces and not on the surrounding basin walls (Figure 18), as would be expected from wave erosion (alternative 2); however, the poor consolidation of the deposit may make it particularly susceptible to wave attack, and the lower gradient of the deposit relative to the crater walls may help to preserve the deposit steps against later erosion by mass wasting.

[48] *Malin and Edgett* [2003] suggested that stepped deposits "appear to be the result of mass movements rather than fluvial processes, with the concentric steps resulting from successive surges of the material as it moved out of the valley or, more likely, as the expression of compressive stress in the material as it came to rest in the crater." The occurrence of successive debris flows (alternative 3) forming so uniform a series of retreating steps (Figure 18d) would be extraordinary. Successive, variable surges of fluvial material might produce a segmented fan, but this mechanism creates distal secondary fans or concave breaks in slope between segments, rather than abrupt scarps bounding the individual segments [*Cooke et al.*, 1993, p. 179; *Ritter et al.*, 1995, p. 250]. Individual debris flows on fans typically form lobate, branching flows with distinct levees, each of which occupies small portions of the deposit. Typically the individual events are of varying size, so that the resulting fan becomes a complex pattern characterized by numerous, relatively narrow, overlapping lobes [*Cooke et al.*, 1993, pp. 171–174].

[49] Secondary explanations for the scarps include (4) a structural origin [*Malin and Edgett*, 2003] or (5) origin by aeolian erosion of differentially resistant layers. Compressive stress in a fan might result in slumping (alternative 4), but we observe a convex outer margin to the deposit scarps rather than concave theater head scarps, which are characteristic of slope failures. Subaerial fans form by aggradation of individual distributaries and avulsion to a new flow path, so layering in these deposits consists of discontinuous lenses, and one would not expect aeolian erosion of differ-

**Figure 14.** Scarp-fronted deposits (white arrows) with no evident distributary channels. These deposits have valley networks that supplied them, but they occur at the ends of entrenched, steep, pristine lower reaches. (a) Deposit in an impact crater located on the northern side of Hellas basin [see also *Howard et al.*, 2005]. (b, c, and d) Deposits within enclosed basins in Aeolis/Nepenthes Mensae fretted and knobby terrains. These deposits along the dichotomy boundary were emplaced after the fretted and knobby terrains formed, likely during the Early Hesperian Epoch. Deposits in Figures 14c and 14d occupy the same basin and share a common altitude of the fan surface above the scarp head. Reference image numbers, locations, and literature references are given in Table 1.

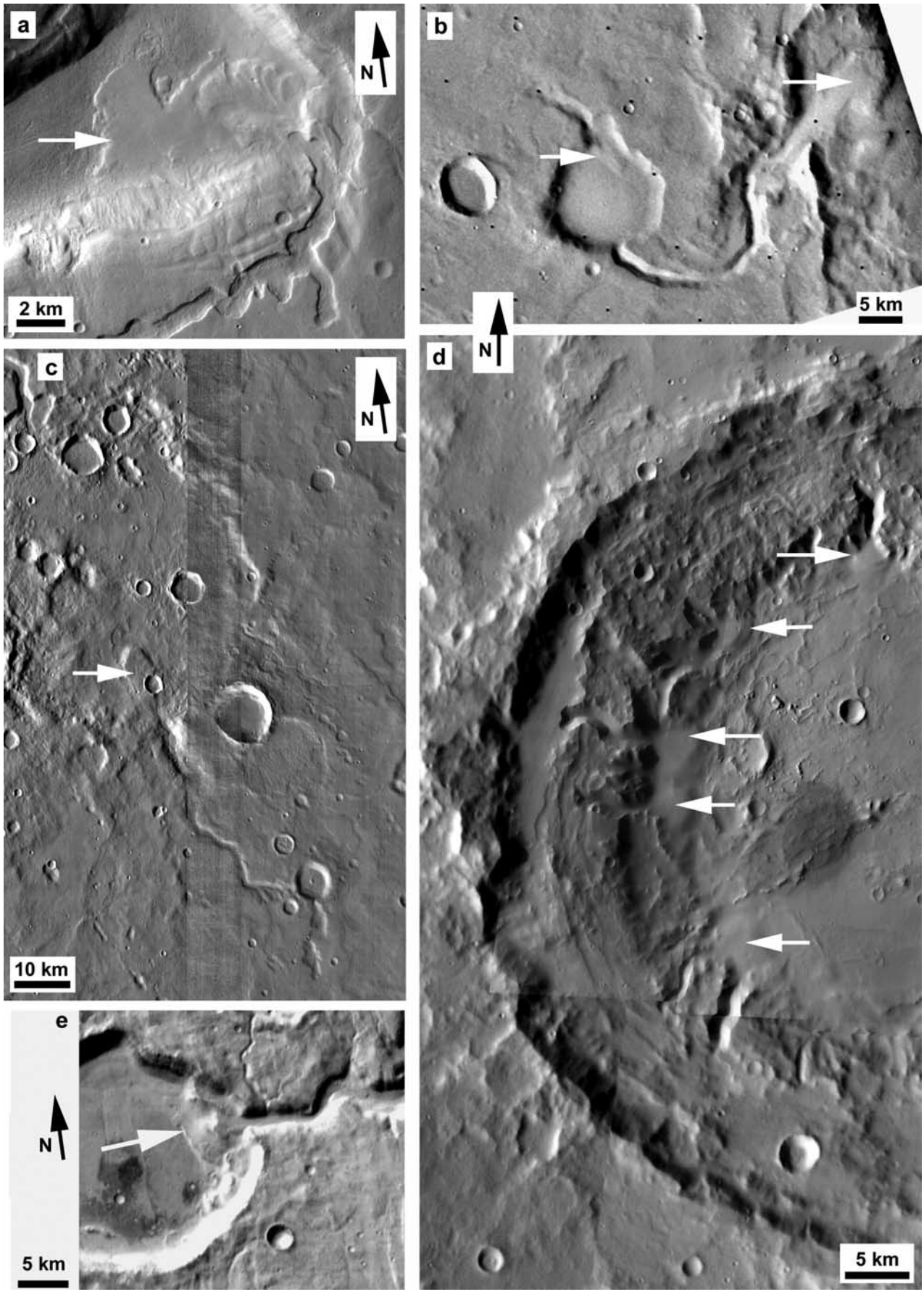


**Figure 15**

entially resistant layers (alternative 5) to produce a scarp around the entire fan circumference (the distal end of an underwater littoral fan, produced by hemipelagic settling, may have more continuous bedding [*Cohen*, 2003, p. 199]). Furthermore, wind-eroded terrains tend to be more feature-rich at small length scales. We have included stepped deposits with deltas as the observations above support a lacustrine rather than secondary origin for the scarps, but it is uncertain whether the deposits formed by shoreline erosion or as stacked fan deltas. *Weitz et al.* [2004] recently reported a deposit in Coprates Catena (Valles Marineris, not shown) that is similar in morphology to that in Figure 18d. These deposits are similarly undissected and suggest emplacement during a single episode of flow that entrenched their source valleys, but subsequent flows were not available to dissect the deposit scarps.

## 4. Valley Longitudinal Profiles Across the Dichotomy Boundary Scarp

[50] At some sites, the age of valley network activity can be established using crosscutting relationships with more extensive terrains of known age. Crater counts and geologic mapping suggest that fretted terrain along the dichotomy boundary developed during the Early Hesperian Epoch in materials of Late Noachian age [*Tanaka*, 1986; *Maxwell and McGill*, 1988; *McGill*, 2000, 2002]. Although some valley networks cross into the fretted terrain (Figures 10 and 19), they terminate abruptly near the dichotomy boundary scarp, and little erosion by running water has occurred on materials located north of the boundary. The Aeolis and Nepenthes Mensae fretted plateau and knobby terrains are located near the equator and are in a superior state of preservation relative to fretted and knobby terrains north of Arabia Terra [*Irwin et al.*, 2004b], which have been extensively modified by ice-facilitated mass-wasting [*Squyres*, 1978; *Lucchitta*, 1984; *Mangold*, 2003]. In this equatorial region, several wide, flat-floored highland valleys (indicating long-term base-level stability or increase) are hanging with respect to the fretted terrain troughs, but the lower reaches of these hanging valleys exhibit prominent knickpoints and short, narrow interior canyons that reach the lower base levels of the fretted terrain floors (Figure 19). The wide upper reaches originally formed before the fretted terrain was fully developed, and later scarp backwasting along the dichotomy boundary left the wide valley floors hanging over 1 km above the knobby terrain basins [*Irwin et al.*, 2004b]. Several of the incised lower reaches terminate in pristine scarp-fronted deposits, which exhibit little or no fan-head trenching or incision of the outer bounding scarp (Figures 14b–14d). These observations along the Aeolis Mensae dichotomy boundary all suggest a brief reactivation of valley networks after the fretted terrain formed and the Gale crater fill was eroded. To be consistent with the lack of fan-head trenching or incision of the outer scarps of these deposits, the reactivation likely consisted of a single discrete epoch of flow, perhaps including multiple flow episodes of similar magnitude. Given the small area of valleys that were entrenched during this epoch, precise dating cannot be accomplished with crater counts, but the relationship to the knobby and fretted terrains suggests that the incision occurred during or after the Early Hesperian. Mamers Vallis, the largest valley that debouched into fretted terrain on Mars (Figure 10), also formed by the end of the Early Hesperian [*McGill*, 2000].

## 5. Interior Channels Within Valley Networks

[51] Channels are excellent indicators of the most recent dominant discharge, as channel form adapts to flow and sediment supply over very short geologic timescales [*Knighton*, 1998, p. 154]. *Irwin et al.* [2005] identified interior channels within 21 valley networks across the Martian highlands and estimated discharge $Q$ ($m^3/s$) using an empirical function of channel width $W$ (m) [*Osterkamp and Hedman*, 1982]:

$$Q = 1.9W^{1.22}. \quad (1)$$

The lower gravity on Mars yields lower mean flow velocity, which is accommodated by ~25% greater width and ~17% greater depth of channels per unit discharge, thus results from equation (1) must be multiplied by a factor of 0.76 to correct for gravity ($1.25^{-1.22} = 0.76$) [*Irwin et al.*, 2005]. Width/depth ratios vary significantly with bank resistance, but equation (1) yields a conservative discharge estimate as it assumes a wide, shallow, sand-bed channel with poorly resistant sand or silt banks. Larger drainage basins on Mars yield larger channels, but estimated runoff production rates (discharge per unit contributing area) decrease with increasing area, as occurs in terrestrial drainage basins due to storage effects and the small size of storms relative to drainage basin area. Smaller subsequent flows were not available to reduce the width and increase the sinuosity of the channels, as occurs in terrestrial rivers after unusually large floods.

[52] The raised channels identified by *Malin and Edgett* [2003] and *Moore et al.* [2003] on the Northeast Holden or "Eberswalde" (provisional name) deposit surface are consistent with other data in terms of channel width relative to contributing area [*Moore et al.*, 2003; *Irwin et al.*, 2005]. This deposit offers several independent means of estimating discharge, however, all of which produce consistent results. We establish here that significant runoff production rates

**Figure 15.** Scarp-fronted deposits (white arrows) with no evident distributary channels. (a) A complex segmented deposit in a fretted valley in Arabia Terra, with part of the contributing theater-headed valley network. Note the entrenchment of the fan head, which may reflect entrenchment of the contributing valley or declining base level within the fretted valley. (b and c) Deposits within impact craters sourced from basin B5 along the Naktong/Scamander/Mamers valley network (Figure 10). Figure 15c shows the head of Mamers Vallis in the lower right corner. The valley descends to the northwest, where it crosscuts a crater, leaving an elevated deposit without dissecting the crater floor. (d) Five deposits at the ends of deep gullies within a 68-km crater in Arabia Terra. This crater floor is the lowest-lying surface within a 700 km radius, so these deposits may reflect a groundwater table at ~−4000 m altitude. (e) Scarp-fronted deposit in the Thaumasia Highlands. Reference image numbers, locations, and literature references are given in Table 1.

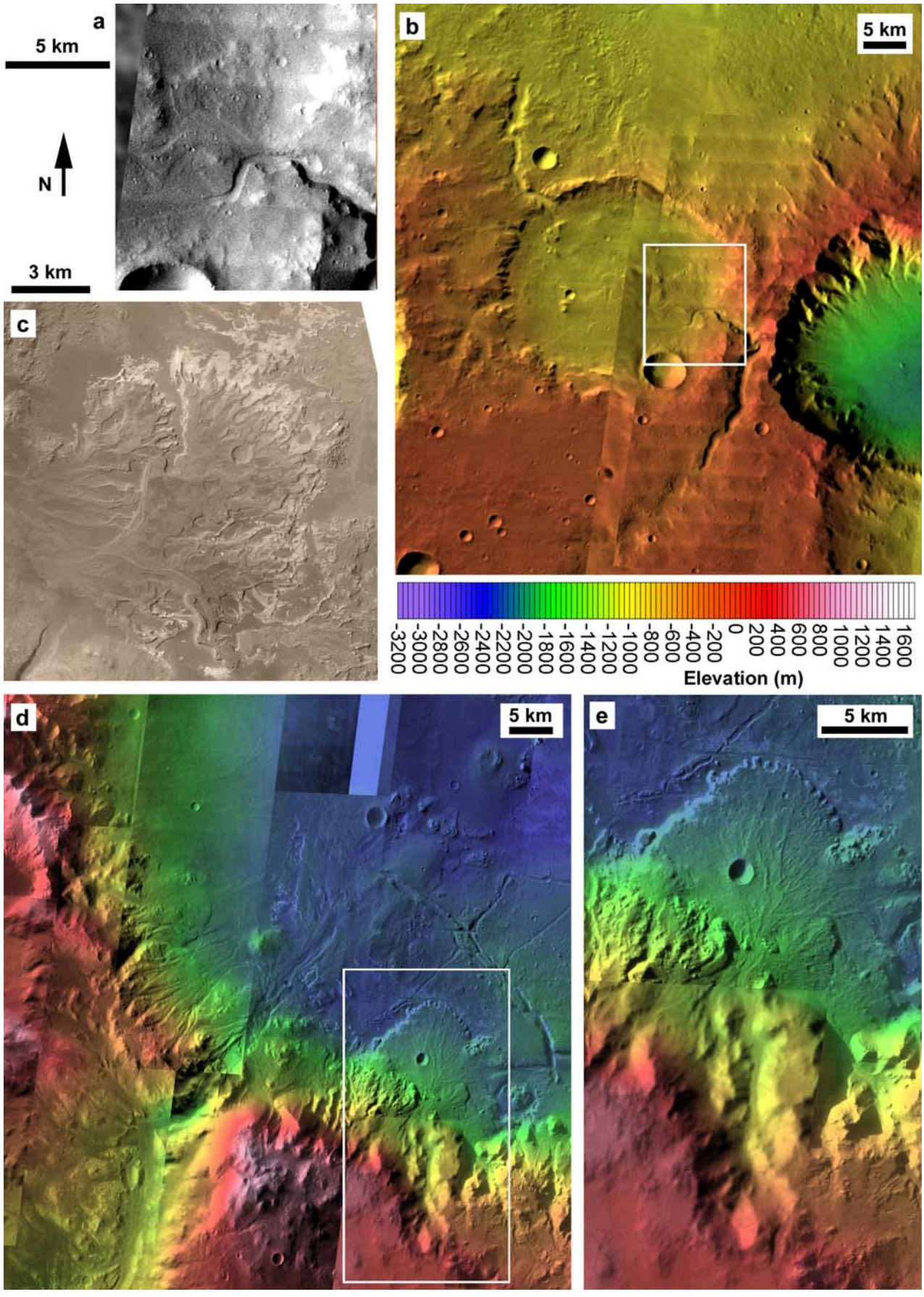
a
5 km
N
3 km
b
5 km
-3200
-3000
-2800
-2600
-2400
-2200
-2000
-1800
-1600
-1400
-1200
-1000
-800
-600
-400
-200
0
200
400
600
800
1000
1200
1400
1600
Elevation (m)
c
d
5 km
e
5 km

**Figure 16**

ended very abruptly by demonstrating that this is very likely a delta [*Moore et al.*, 2003; *Bhattacharya et al.*, 2005] rather than an eroded riverine fan, as proposed by *Jerolmack et al.* [2004], and by confirming the modeled discharge and runoff production rates using additional methods.

[53] Given the average 130-m width of the inverted channels, equation (1) yields a discharge estimate of 550 $m^3/s$, which is comparable to the 700 $m^3/s$ result that *Moore et al.* [2003] obtained with a somewhat less conservative function similar to (1). *Jerolmack et al.* [2004] obtained 410 $m^3/s$ using a model for equilibrium shape of channelized alluvial fans, and they estimated a minimum time of origin at "several decades to centuries" if the flow was constant at 410 $m^3/s$, or perhaps a factor of 20 greater longevity if the channel-forming flow was present only 5% of the time. In terrestrial rivers, *Nanson and Croke* [1992] established that non-cohesive floodplains developed primarily by lateral point bar accretion where unit stream power $\omega$ was between about 10 and 60 $W/m^2$, beyond which straighter braided channels begin to dominate. Stream power per unit width is calculated as

$$\omega = \rho g Q S / W, \tag{2}$$

where $\rho$ is fluid density (1000 $kg/m^3$), $g$ is gravitational acceleration (3.72 $m/s^2$), and $S$ is the channel slope (measured at 0.006 from MOLA data by *Jerolmack et al.* [2004]). Unit stream power for the "Eberswalde" channel is 70 $W/m^2$ given a discharge of 410 $m^3/s$, a reasonable agreement.

[54] *Komar* [1980] and *Komatsu and Baker* [1997] showed the relationship between bed shear stress $\tau$ ($N/m^2$) and the grain diameters that would be transported as bed, suspended, and wash load on Mars. Shear stress is calculated as

$$\tau = \rho g H S, \tag{3}$$

where $H$ is the flow depth. The depth can be calculated from discharge and measured width by a combination of the continuity and Manning equations:

$$Q = HWV = H^{5/3} S^{1/2} g^{1/2} W n^{-1}, \tag{4}$$

where $V$ is mean flow velocity, and Manning's roughness coefficient $n$ is taken to be 0.035 (the natural variability of this coefficient, plus or minus a factor of $\sim$2, does not significantly affect our results). We find that the flow depth of 1.6 m yields a bed shear stress of 37 $N/m^2$, which could transport particles $\sim$3–110 mm in diameter as bed load and particles smaller than $\sim$3 mm as suspended load. These results show that the overbank (suspended load) deposits should be susceptible to aeolian deflation, whereas the channel floor deposits should be a resistant lag, so the occurrence of inverted channels here is consistent with models of fan hydrology. Wind cannot transport grains >2–4 mm in diameter, and the preserved scroll bar texture of the channels indicates negligible post-depositional weathering of the bed material, so these results falsify the *Jerolmack et al.* [2004] hypothesis that wind could have removed both the lower channel fill and overbank deposits of a previously more extensive fan. Rapid water loss down-fan would result in an outward fining of grain size, but this scenario seems inconsistent with the gradual meander development, which requires persistent flow that is filling the channel more slowly [*Bhattacharya et al.*, 2005]. *Jerolmack et al.* [2004] note wind-eroded materials on the crater floor inward from the fan's peripheral scarp, which they suggested might be remnants of a previously more extensive fan, but no unique distinction can be made between this proposed origin and erosion of a deltaic bottomset [*Bhattacharya et al.*, 2005] or airfall deposit.

[55] To avoid forming a lake in "Eberswalde" crater, water would have to be removed from this basin as rapidly as it was delivered. The area of the basin floor below the −1400 m elevation contour, at the front of the deposit's surface, is about 400 $km^2$, so the nearly constant channel-forming groundwater discharge of 410 $m^3/s$ suggested by *Jerolmack et al.* [2004] would increase the lake level by up to 32 meters per terrestrial year. This water must have been removed from the basin as rapidly as it was delivered, however, as the water surface must be relatively stable to develop laterally accreting point bars on the delta surface. Pan evaporation rates are less than 10 meters per year even in the warmest and most arid terrestrial deserts, and evaporation from lakes is typically only 0.7 times the pan evaporation rate [*Farnsworth et al.*, 1982], so very rapid water loss by infiltration would be required to avoid forming a lake. The occurrence of large springs at higher elevations in a watershed and high infiltration rates at lower elevations is questionable in a hypothetical environment without precipitation, although one might envision special circumstances that would make this hydrologic model viable. We also find no indication that a layer of surface ice ever occurred in this area, as we see no landform degradation by ice-facilitated creep, which is common in higher latitudes [*Jankowski and Squyres*, 1993]. We support the conclusions of *Moore et al.* [2003] and *Bhattacharya et al.* [2005] that a paleolake likely occurred in "Eberswalde" crater (*Malin and Edgett* [2003] also suggested a lake as a possibility), because deflation cannot explain the terminal scarp given the consistently modeled discharges and sedi-

**Figure 16.** Valley-terminal deposits with evident distributary channels in Margaritifer Sinus. (a) Scarp-fronted distributary fan in a 25-km crater located on the southern margin of Parana basin. (b) Setting of Figure 15a (inset box), colored with MOLA topography, showing the fan located at the end of a pristine, entrenched lower reach of a valley network. An exit breach in the northwestern side of the crater was likely responsible for lowering the base level within the crater, allowing the active channel to entrench the fan surface. (c) Distributary fan of inverted channels in "Eberswalde" crater (MOC image mosaic provided by Malin Space Science Systems). (d) Deposits on the southwestern floor of Holden crater. Large alluvial fans in the northwestern corner of the image (green shade) have toes that are concordant with the crater floor. At the center of the image is the lobate terminal deposit for Uzboi Vallis, which enters the crater from the southwest. The inset box shows the location of Figure 16e, a scarp-fronted distributary fan or delta that was supplied from a dissected alcove in the crater wall. Reference image numbers, locations, and literature references are given in Table 1.

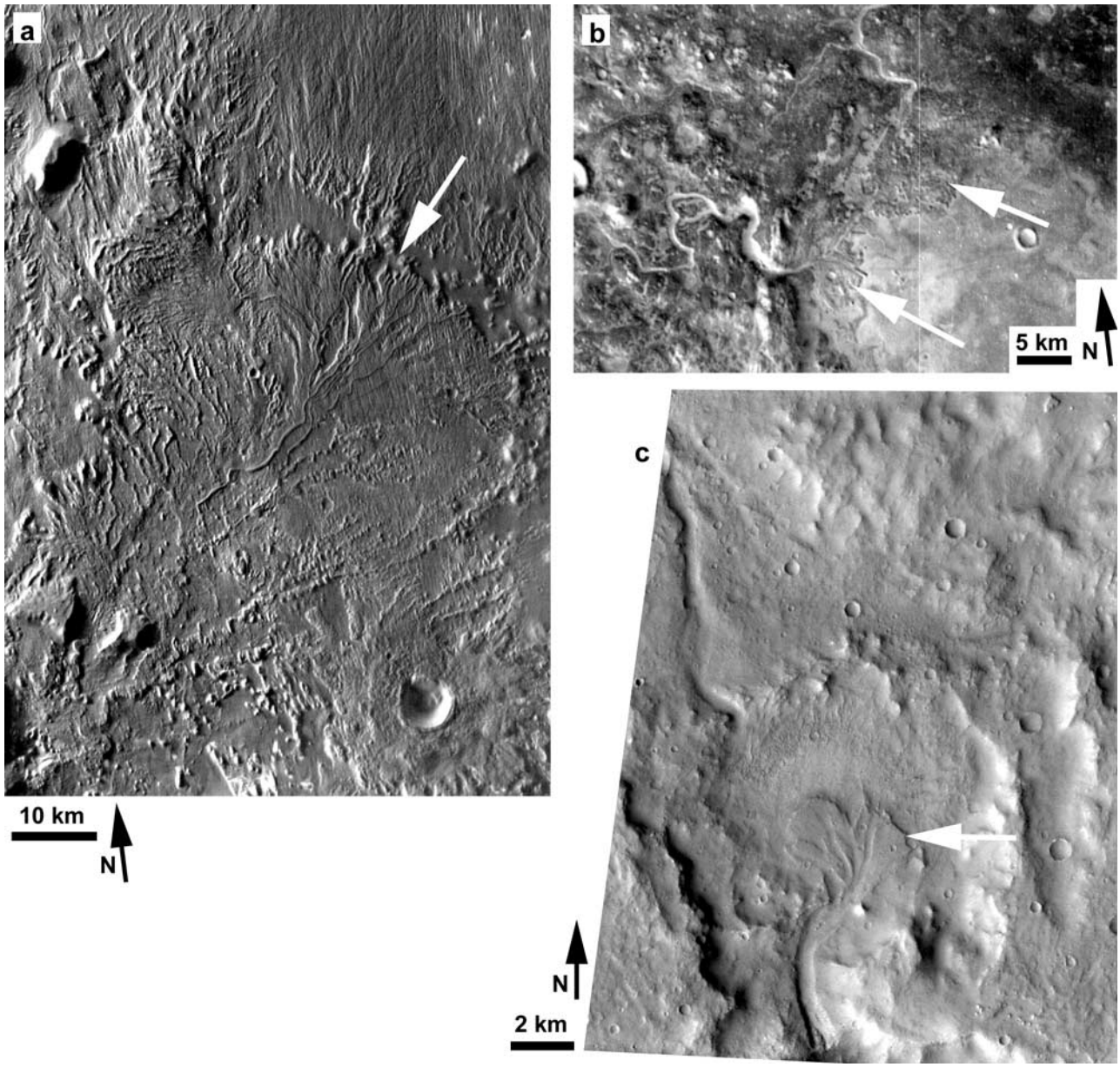


**Figure 17.** Scarp-fronted fans (white arrows) with distributary channels in (a) Aeolis Mensae, (b) a crater in the Nili Fossae region, and (c) a crosscut crater in Margaritifer Sinus, where flow was toward the north. The craters in Figures 17b and 17c have outlet valleys, but little to no entrenchment of the deposits occurred with falling base level in the crater. Distributary channels occur in inverted relief in Figures 17a and 17b. Reference image numbers, locations, and literature references are given in Table 1.

ment grain sizes, and a more constant groundwater discharge would require the presence of a lake as no reasonable mechanism is available to remove water from the closed basin at a constant 410 $m^3/s$ rate. This discharge indicates a runoff production rate of ~1 cm/day from the ~4800 $km^2$ drainage basin, and this discharge must have declined very abruptly to avoid dissecting the fan surface as the lake level fell. In this enclosed basin, the discharge must have been persistent, although perhaps variable as are terrestrial rivers, to maintain a relatively stable lake level long enough to develop the uppermost layer of the deposit. *Bhattacharya et al.* [2005] estimated that the surface layer would require something on the order of several thousand years to develop, with the entire deposit forming in ~150,000 years. This age range is consistent to an order of magnitude with the time required to develop large alluvial fans in some Martian craters [*Moore and Howard*, 2005]. The actual duration of this late epoch of fluvial activity depends on the flood frequency, which is unknown.

## 6. Discussion and Conclusions

[56] In this paper we describe evidence for a late epoch of relatively abundant runoff on early Mars, when fluvial erosion rates temporarily exceeded the slower but longer-term degradation of impact craters that characterized most

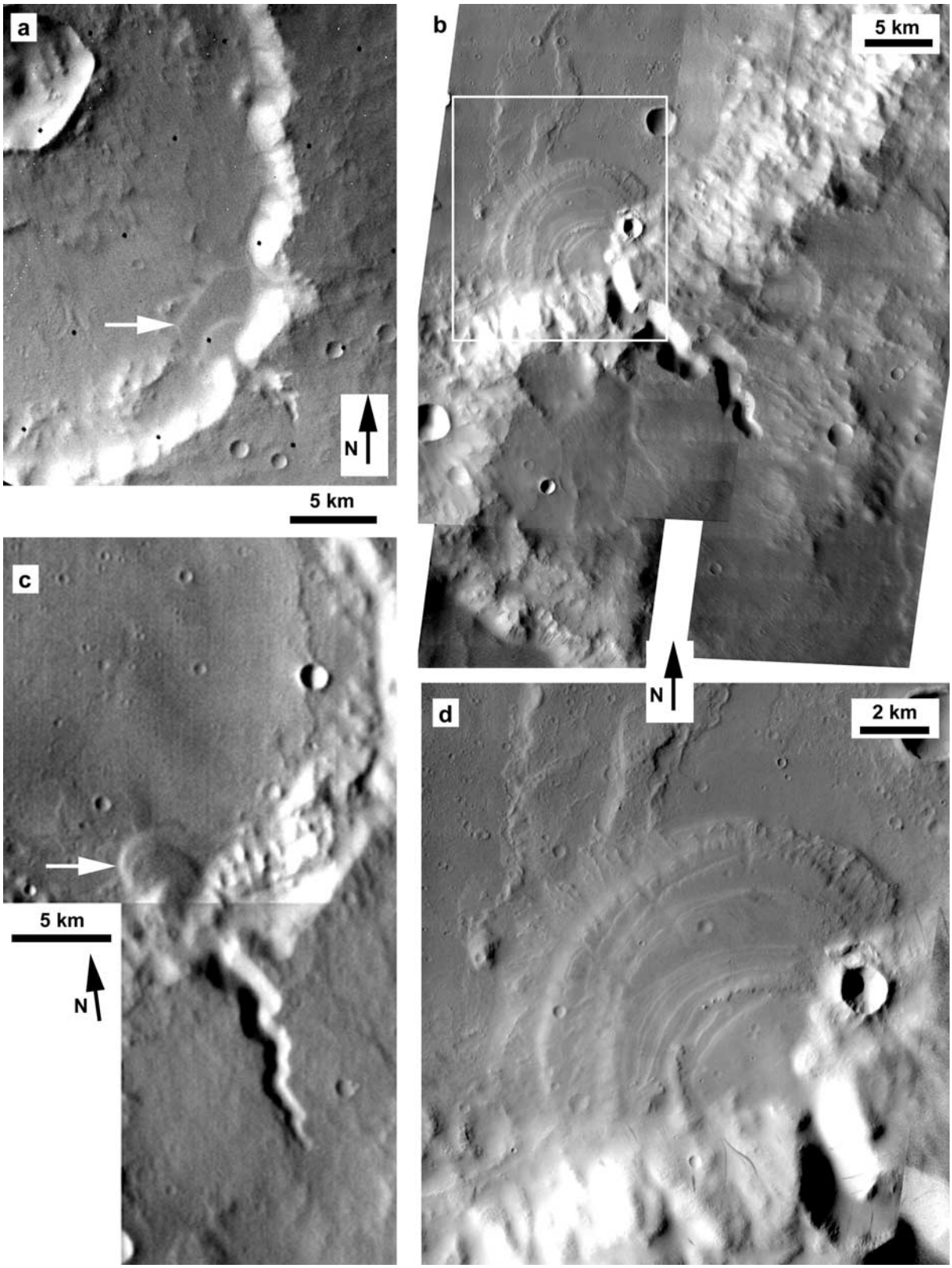


**Figure 18.** (a–c) Valley-terminal deposits with stepped surfaces in Memnonia. Note the pristine, stubby source valleys, which may have received drainage from shallow basins above the valley heads. The multiple bounding scarps are undissected and show that no erosion of the deposit occurred under a lower base level control after deposition. (d) Enlargement of the deposit shown in the inset box in Figure 17b. One of the scarps near the top of the fan in Figure 18d has positive relief and is knobby. Although difficult to interpret uniquely, this feature may represent a resistant outcrop of underlying rocks. Reference image numbers, locations, and literature references are given in Table 1.

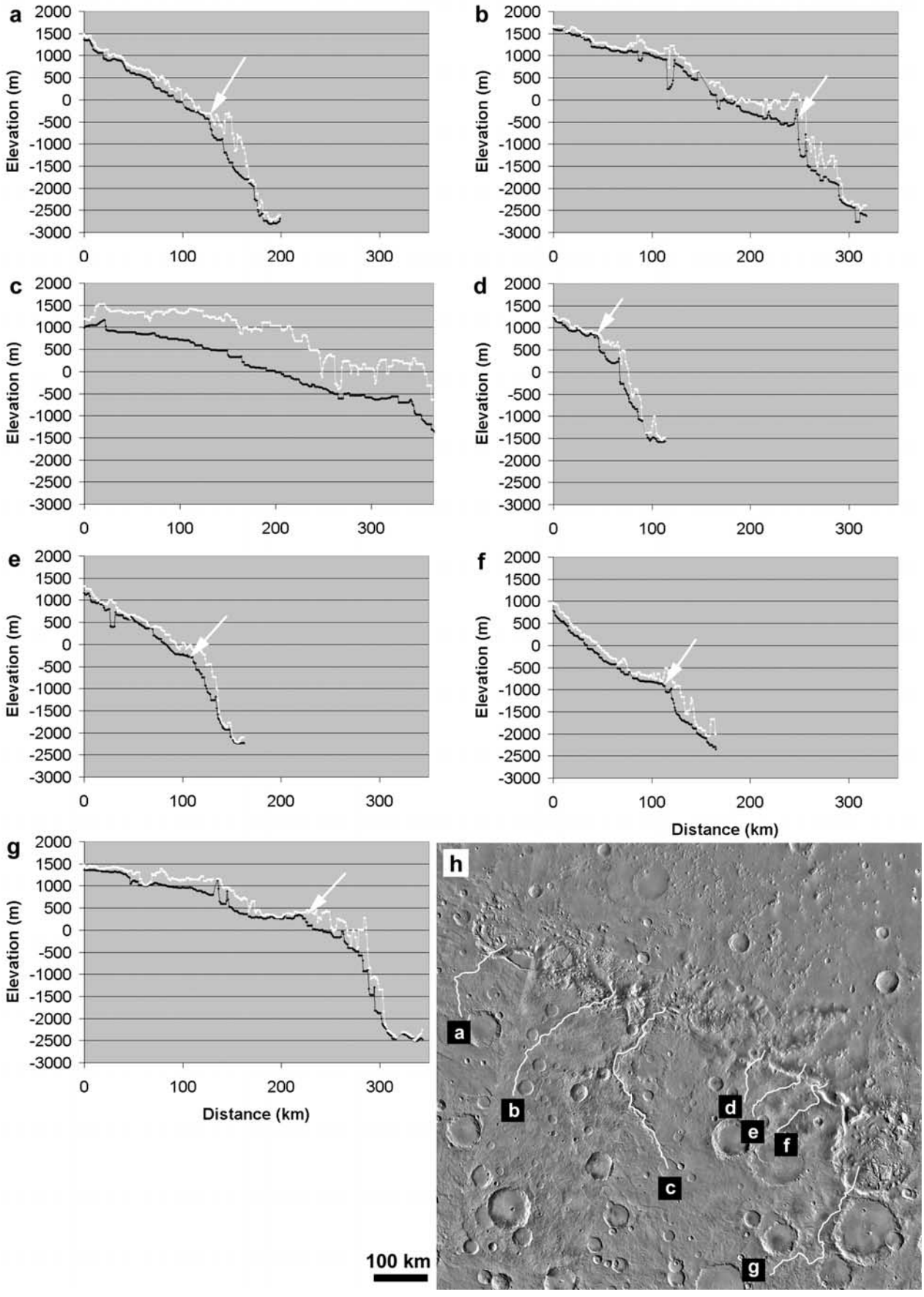
a
b
c
d
e
f
g
h
Elevation (m)
2000
1500
1000
500
0
-500
-1000
-1500
-2000
-2500
-3000
0
100
200
300
Distance (km)
100 km

**Figure 19**

of the Noachian Period. Valley networks that formed during this late epoch have immature characteristics due to the brevity of Earthlike runoff production rates rather than to differences in the primary water source between Earth and Mars. We use the term "epoch" for a discrete period of activity bounded by periods of inactivity, but the precise timing and duration of the epoch are poorly constrained, and flows may have been variable or intermittent during that time [*Moore et al.*, 2003; *Jerolmack et al.*, 2004; *Fassett and Head*, 2005; *Moore and Howard*, 2005; *Bhattacharya et al.*, 2005; *Howard et al.*, 2005]. The intensive erosion appears to have occurred over parts of the Late Noachian and Early Hesperian geologic epochs [*Tanaka*, 1986], so the epoch of intense fluvial erosion does not correspond to a previously defined interval of time. The supporting evidence described in this paper includes the following:

[57] 1. In Gale crater, a terraced crater in Memnonia, and in several places along the Naktong/Scamander/Mamers valley network, we find pristine, V-shaped entrance and/or exit breaches in basins that previously had been extensively modified without overflowing. In order to maintain this narrow, V-shaped valley morphology with little to no sidewall dissection, geologically rapid incision of the rim must have occurred shortly before fluvial activity ended altogether. Many other examples of late-stage entrenchment occur on Mars [e.g., *Baker and Partridge*, 1986; *Howard et al.*, 2005], but we use these as type examples. In a 46-km crater along the Herschel/Gale valley network and at an unnamed crater in Terra Sirenum, we find late-stage entrenchment of an earlier, higher crater outlet, so that a terrace now occurs in the outlet valley. The outlet elevations may have been previously maintained at the terrace level by aggradation of the outlet valley floor by widening during relatively arid intervals between throughflows. Entrenched inlet or outlet valleys commonly have few or no tributaries near the crater rim and no sidewall dissection, but in each of the studied cases a large source valley network occurs in the highlands to the south of the breached basin. These breaches suggest a temporary increase in the water budget shortly before flows in valley networks declined permanently.

[58] 2. Of the 33 positive-relief valley-terminal deposits (putative deltas) known to us at the time of writing, 14 were derived from valley networks that show signs of late-stage entrenchment, 11 were derived from shorter incised valleys that have shallow enclosed basins above the valley head (most of these head basins received drainage from upslope), five were sourced from large gullies within a deep impact crater in Arabia Terra, and three were derived from stubby contributing valleys with indeterminate source areas. This late entrenchment and valley-terminal deposition were likely contemporary and related to an increase in flow [*Howard et al.*, 2005]. Only two of the 33 putative deltas we examined show deep entrenchment of the peripheral scarp, so the deposits' morphology does not suggest a prolonged, slow climatic decline with a falling base level. In one of the two cases where the frontal scarp of the deposit is entrenched (#27 in Table 1, Figure 16b), incision of the deposit was likely related to incision of the crater's outlet valley during peak flow conditions. These scarp-fronted deposits appear to have formed during a single, terminal epoch of valley network activity, which ended abruptly. The lack of deltas in most breached craters is suggestive of ephemeral flows and instability of lake level.

[59] 3. Erosive fluvial activity occurred both before the Gale impact (which is tightly constrained stratigraphically to near the Noachian/Hesperian boundary) and after the crater was buried and exhumed by aeolian processes in the Early Hesperian. Some highland valley networks have incised to low base levels in Early Hesperian fretted terrain, which appears to have developed by a suite of processes unrelated to precipitation runoff [*Irwin et al.*, 2004b]. The crosscutting relationships and interposition of fluvial, impact, and aeolian landforms in these dichotomy boundary study areas may reflect intermittent valley network activity, including at least one hiatus in the erosive fluvial activity near the Noachian/Hesperian boundary. As in terrestrial arid climates, precipitation may have been more abundant at higher altitudes than in lower-lying fretted terrains.

[60] 4. *Irwin et al.* [2005] identified channels within 21 valley networks across the Martian highlands and showed that these channels record significant (Earthlike) runoff production rates near the end of fluvial activity on Mars. However, the flows appear to have declined abruptly, as smaller subsequent flows were not available to reduce the width and increase the sinuosity of the channels. As a case study, we use three alternative methods based on channel morphometry to establish mutually consistent channel-forming discharge estimates for an inverted channel in "Eberswalde" crater, and we describe how the grain diameters transported as channel bed and overbank suspended load in this regime favored the subsequent development of inverted topography. Finally, we describe the difficulties inherent to producing a scarp-fronted fan from a previously more extensive deposit given the size of the transported bed load in this regime.

[61] *Baker and Partridge* [1986] originally recognized the entrenchment of lower reaches of some valley networks, which they attributed to a late stage of sapping along older degraded valley floors. Although their observation of late entrenchment appears valid, the sapping hypothesis is challenged by several features of these valleys. Incision of crater exit breaches by headward sapping would require long-lived paleolakes in the craters, because no other aquifer is available above the outlet valley heads. Such prolonged flooding would require an abundant water supply to the basins, which seems inconsistent with an origin of the

**Figure 19.** (a–g) Longitudinal profiles of the major valleys that debouch into Aeolis and Nepenthes Mensae. Black lines indicate the valley thalwegs, and white lines approximate the surrounding surface. Note that all valleys exhibit an abrupt convex break in slope (white arrows) at the dichotomy boundary, where deep, narrow lower reaches are entrenched. This observation suggests poor grading to fretted terrain base levels and likely a brief period of flow during or after the fretted terrain development. (h) Locator map from the Viking MDIM 2.1 showing the locations of these profiles. Figure 12 of *Irwin et al.* [2004b] provides a detailed view of the valley in Figure 19f, and Figures 14b and 14d show the ends of valleys plotted here as Figures 19a and 19g, respectively.

crater outlets exclusively by sapping. The Aeolis Mensae fretted terrain and the Gale crater interior mound appear to have developed during a hiatus in valley network activity [*Irwin et al.*, 2004b], so a mechanism would be required to raise the water table at the end of this hiatus. Valleys interpreted as sapping-related typically have stubby tributaries, are often structurally controlled rather than sinuous, are often not V-shaped in cross section, and might be expected at more than one site along a large crater's circumference [e.g., *Dunne*, 1980]. The pristine lower reaches on Mars are localized and widely separated by tens to hundreds of kilometers, which would be difficult to explain if northward groundwater flow were responsible. Overland flow along pre-existing topography can explain the locations of these entrenched lower reaches, but if a declining water table were responsible, we would expect them to be concentrated more along scarps, including crater walls and the dichotomy boundary. Interior channel morphology [*Irwin et al.*, 2005] and the lack of late-stage dissection of most of the putative delta surfaces supports a rapid decline in runoff, not a gradual one as would be expected from a transition to sapping. Finally, some of the entrenched theater-headed valleys originate at high altitudes adjacent to deep impact craters, and it is more likely that groundwater would originate first in the crater than at the elevated valley head [*Howard et al.*, 2005].

[62] A more viable explanation relies on an epoch of relatively intense runoff, concentrated in higher elevations as in terrestrial deserts, which could fill and overflow previously enclosed basins. Prior to this late-stage erosion, Noachian highland gradation and degradation/loss of impact craters occurred when the ratio of precipitation/(evaporation + infiltration) was initially low [e.g., *Grant and Schultz*, 1993; *Grant*, 2000], so that fluvial erosion was effective primarily on steeper intracrater or intercrater surfaces. This light, localized, and/or ephemeral runoff would act as a scale-inefficient process over long distances, along with aeolian sand transport, to smooth the intercrater plains without producing mature concave drainage basins. As an alternative hypothesis, it is possible that the earliest runoff was abundant at times but infrequently so, allowing creep, impact gardening, and aeolian processes to fill valley networks as rapidly as they could form on low-gradient surfaces. This alternative is not particularly appealing, however, as the competing processes would have to be at least as effective as fluvial erosion in redistributing material, at least on low slopes, and they should therefore have a more profound expression in degraded crater morphology than has been observed in the equatorial highlands.

[63] The hundreds of meters of Noachian denudation that was required to degrade and fill impact craters at the observed rates [*Craddock and Maxwell*, 1993; *Craddock et al.*, 1997] could be accomplished in the terrestrial environment on the order of millions of years, far less than the ~200 million years or more during which crater degradation occurred on Mars. This modification must have been a long-term (although possibly punctuated) process throughout the Middle and Late Noachian Epochs, however, as similarly sized, adjacent impact craters are often degraded to very different forms (Figure 1a). Martian valley networks are immature relative to their terrestrial counterparts, and their short length, low drainage density, and the poor grading of their drainage basins suggest slow process rates or a relatively brief time for development [*Carr and Clow*, 1981; *Stepinski et al.*, 2004]. However, the spatial ubiquity of crater degradation (not just on valley floors), the unique association between degraded crater form and fluvial processes [*Craddock et al.*, 1997; *Forsberg-Taylor et al.*, 2004], the ineffectiveness of wind in modifying rocky surfaces on Mars [*Golombek and Bridges*, 2000; *Grant et al.*, 2005], the origin of valley networks near sharp drainage divides [e.g., *Irwin and Howard*, 2002], the need for recharge to support erosion of valley network volumes [*Howard*, 1988; *Goldspiel and Squyres*, 1991; *Grant*, 2000; *Gulick*, 2001], the runoff production rates indicated by channel dimensions [*Irwin et al.*, 2005], and new Mars Exploration Rover geochemical results [*Squyres et al.*, 2004] require that early Mars was warmer and wetter than it is at present. Precipitation was very likely responsible for valley networks and crater degradation, but truly Earthlike, humid conditions must have been short-lived and punctuated by drier periods.

[64] We can only speculate on the cause of the late fluvial activity, which may have followed an impact (leaving a relatively fresh crater of the appropriate age) [*Colaprete et al.*, 2005] or outflow channel activity [*Baker et al.*, 1991; *Mangold et al.*, 2004]. Higher precipitation rates and more erosive flows may have occurred over time due to accumulation of a thicker atmosphere, supported by volcanic outgassing (Tharsis and other volcanic provinces were developing during this time [*Tanaka*, 1986; *Phillips et al.*, 2001]), inhibition of carbonate deposition due to the low pH maintained by volcanic $SO_2$, and reduced expulsion of the atmosphere by impacts. If above-freezing temperatures usually followed impacts [*Segura et al.*, 2002; *Colaprete et al.*, 2005], then one would expect variability in precipitation rates, which depend on temperature. Alternatively, reduced infiltration capacity due to permafrost or duricrust development could support higher runoff production even if the total precipitation did not increase with time [*Howard et al.*, 2005]. Given more precipitation and/or reduced infiltration capacity, the Late Noachian "degraded" valley networks [*Baker and Partridge*, 1986] were entrenched into this older geomorphic surface, but the rivers visibly had inadequate time and resources to fully extend their small tributaries and to regrade the highlands to an Earthlike set of quasi-equilibrium drainage basins. This incomplete entrenchment left the characteristic undissected interfluves between valleys. Finally, the "pristine" valleys formed by entrenchment of lower reaches and overflow of previously enclosed basins during the last part of this late epoch of erosion. High-resolution imaging shows that the cuspate "headwalls" of many valley branches have shallow upslope tributaries (Figures 2b, 2c, 4b, 13a, and 16b), suggesting that the scarps may be knickpoints related to late entrenchment rather than sapping headwalls.

[65] An unresolved issue related to timing remains. The preserved landforms described here record the last major fluvial modifications within their respective drainage basins, and observations suggest a consistent erosional history and sudden decline across widely separated areas. However, these valleys may not all be precisely contemporary or coeval with pristine-appearing valleys described elsewhere by other authors [e.g., *Baker and Partridge*, 1986; *Mangold*

*et al.*, 2004; *Williams et al.*, 2005]. Even within a single valley network incised into a surface of known stratigraphic age, such as the terraced crater in Memnonia, the morphologically distinct contributing and outlet valleys may have formed at different times because the crater did not initially overflow. Reactivation of a valley at intervals of time could complicate dating its initial incision. Issues with small crater populations, particularly on narrow valleys [*Malin*, 1976], can confound such age determinations for small drainage basins. The stratigraphic age of most "degraded" Martian valley networks and degraded craters is constrained generally to the Noachian Period by counts of larger, superimposed fresh craters [e.g., *Craddock and Maxwell*, 1990; *Irwin and Howard*, 2002], but valley reactivations and some new valley development appear to have occurred during the Hesperian, or even locally during the Amazonian [e.g., *Carr*, 1996, p. 79–80; *Mangold et al.*, 2004]. The prospect of multiple regional fluvial episodes cannot be uniquely discounted; however, the characteristics of terminal valley activity appear to be similar across much of Mars. Furthermore, fluvial erosion on Mars is a global problem, requiring a change in global air temperature and pressure relative to the present state, so it is likely that a temporary atmospheric mechanism that allowed flow in one region would also be relevant to a distant valley network.

[66] This scenario is offered as a testable hypothesis that may explain the immature morphology of Martian valley networks given precipitation runoff and prolonged impact crater degradation. The success of a model in explaining observations is no guarantee of its uniqueness, however, and detailed work across many Martian drainage basins is necessary to constrain age relationships and to test and refine this hypothesis.

[67] **Acknowledgments.** This project is a compilation of results funded by separate NASA Mars Data Analysis Program grants to T. A. Maxwell (Evaluation of Possible Lacustrine Features in the Martian Highlands), R. A. Craddock (Age and Characteristics of Martian Valley Networks), and J. M. Moore (Topography and Basin Deposits of the Martian Highlands). We are grateful for the constructive reviews from Keith Harrison and Nicolas Mangold.

## References

Aharonson, O., M. T. Zuber, D. H. Rothman, N. Schorghofer, and K. X. Whipple (2002), Drainage basins and channel incision on Mars, *Proc. Natl. Acad. Sci. U. S. A.*, *99*, 1780–1783.

Arvidson, R. E. (1974), Morphologic classification of Martian craters and some implications, *Icarus*, *22*, 264–271.

Baker, V. R. (1982), *The Channels of Mars*, 198 pp., Univ. of Tex. Press, Austin.

Baker, V. R., and J. Partridge (1986), Small Martian valleys: Pristine and degraded morphology, *J. Geophys. Res.*, *91*, 3561–3572.

Baker, V. R., R. G. Strom, V. C. Gulick, J. S. Kargel, G. Komatsu, and V. S. Kale (1991), Ancient oceans, ice sheets and the hydrological cycle on Mars, *Nature*, *352*, 589–594.

Bandfield, J. L., V. E. Hamilton, and P. R. Christensen (2000), A global view of Martian surface compositions from MGS-TES, *Science*, *287*, 1626–1630, doi:10.1126/science.287.5458.1626.

Bandfield, J. L., T. D. Glotch, and P. R. Christensen (2003), Spectroscopic identification of carbonate minerals in the Martian dust, *Science*, *301*, 1084–1087.

Bhattacharya, J. P., T. H. D. Payenberg, S. C. Lang, and M. Bourke (2005), Dynamic river channels suggest a long-lived Noachian crater lake on Mars, *Geophys. Res. Lett.*, *32*, L10201, doi:10.1029/2005GL022747.

Blair, T. C., and J. G. McPherson (1994), Historical adjustments by Walker River to lake level fall over a tectonically tilted half-graben floor, Walker Lake basin, Nevada, *Sediment. Geol.*, *92*, 7–16.

Cabrol, N. A., and E. A. Grin (1999), Distribution, classification, and ages of Martian impact crater lakes, *Icarus*, *142*, 160–172.

Cabrol, N. A., and E. A. Grin (2001a), Composition of the drainage network on early Mars, *Geomorphology*, *37*, 269–287.

Cabrol, N. A., and E. A. Grin (2001b), The evolution of lacustrine environments on early Mars: Is Mars only hydrologically dormant?, *Icarus*, *149*, 291–328.

Cabrol, N. A., E. A. Grin, H. E. Newsom, R. Landheim, and C. P. McKay (1999), Hydrogeologic evolution of Gale crater and its relevance to the exobiological exploration of Mars, *Icarus*, *139*, 235–245.

Carr, M. H. (1996), *Water on Mars*, 229 pp., Oxford Univ. Press, New York.

Carr, M. H. (1999), Retention of an atmosphere on early Mars, *J. Geophys. Res.*, *104*, 21,897–21,909.

Carr, M. H. (2001), Mars Global Surveyor observations of Martian fretted terrain, *J. Geophys. Res.*, *106*, 23,751–23,593.

Carr, M. H., and F. C. Chuang (1997), Martian drainage densities, *J. Geophys. Res.*, *102*, 9145–9152.

Carr, M. H., and G. D. Clow (1981), Martian channels and valleys: Their characteristics, distribution, and age, *Icarus*, *48*, 91–117.

Carr, M. H., and J. W. Head III (2003), Oceans on Mars: An assessment of the observational evidence and possible fate, *J. Geophys. Res.*, *108*(E5), 5042, doi:10.1029/2002JE001963.

Cohen, A. S. (2003), *Paleolimnology: The History and Evolution of Lake Systems*, 500 pp., Oxford Univ. Press, New York.

Colaprete, A., R. M. Haberle, T. L. Segura, O. B. Toon, and K. Zahnle (2005), The effect of impacts on the Martian climate, in *Workshop on the Role of Volatiles and Atmospheres on Martian Impact Craters*, *LPI Contrib. 1273*, pp. 32–33, Lunar and Planet. Inst., Houston, Tex.

Cooke, R., A. Warren, and A. Goudie (1993), *Desert Geomorphology*, 526 pp., UCL, London.

Craddock, R. A., and A. D. Howard (2002), The case for rainfall on a warm, wet early Mars, *J. Geophys. Res.*, *107*(E11), 5111, doi:10.1029/2001JE001505.

Craddock, R. A., and T. A. Maxwell (1990), Resurfacing of the Martian highlands in the Amenthes and Tyrrhena region, *J. Geophys. Res.*, *95*, 14,265–14,278.

Craddock, R. A., and T. A. Maxwell (1993), Geomorphic evolution of the Martian highlands through ancient fluvial processes, *J. Geophys. Res.*, *98*, 3453–3468.

Craddock, R. A., T. A. Maxwell, and A. D. Howard (1997), Crater morphometry and modification in the Sinus Sabaeus and Margaritifer Sinus regions of Mars, *J. Geophys. Res.*, *102*, 13,321–13,340.

Dunne, T. (1980), Formation and controls of channel networks, *Prog. Phys. Geogr.*, *4*, 211–239.

Edgett, K. S., and M. C. Malin (2001), Rock stratigraphy in Gale Crater, Mars, *Proc. Lunar Planet. Sci. Conf. 32nd*, abstract 1005.

Farnsworth, R. K., E. S. Thompson, and E. L. Peck (1982), Evaporation atlas for the contiguous 48 United States, *NOAA Tech. Rep. NWS 33*, Natl. Weather Serv., Washington, D. C.

Fassett, C. I., and J. W. Head III (2005), Fluvial sedimentary deposits on Mars: Ancient deltas in a crater lake in the Nili Fossae region, *Geophys. Res. Lett.*, *32*, L14201, doi:10.1029/2005GL023456.

Forsberg-Taylor, N. K., A. D. Howard, and R. A. Craddock (2004), Crater degradation in the Martian highlands: Morphometric analysis of the Sinus Sabaeus region and simulation modeling suggest fluvial processes, *J. Geophys. Res.*, *109*, E05002, doi:10.1029/2004JE002242.

Forsythe, R. D., and J. R. Zimbelman (1995), A case for ancient evaporite basins on Mars, *J. Geophys. Res.*, *100*, 5553–5563.

Gaidos, E., and G. Marion (2003), Geological and geochemical legacy of a cold early Mars, *J. Geophys. Res.*, *108*(E6), 5055, doi:10.1029/2002JE002000.

Gaidos, E. J., M. Güdel, and G. A. Blake (2000), The faint young sun paradox: An observational test of an alternative solar model, *Geophys. Res. Lett.*, *27*, 501–503.

Gilbert, G. K. (1890), Lake Bonneville, *Mem. U.S. Geol. Surv.*, *1*, 438 pp.

Goldspiel, J. M., and S. W. Squyres (1991), Ancient aqueous sedimentation on Mars, *Icarus*, *89*, 392–410.

Goldspiel, J. M., and S. W. Squyres (2000), Groundwater sapping and valley formation on Mars, *Icarus*, *148*, 176–192.

Golombek, M. P., and N. T. Bridges (2000), Erosion rates on Mars and implications for climate change: Constraints from the Pathfinder landing site, *J. Geophys. Res.*, *105*, 1841–1853.

Graedel, T. E., I. J. Sackmann, and A. I. Boothroyd (1991), Early solar mass loss: A potential solution to the weak sun paradox, *Geophys. Res. Lett.*, *18*, 1881–1884.

Grant, J. A. (1987), The geomorphic evolution of eastern Margaritifer Sinus, Mars, in *Advances in Planetary Geology*, *NASA Tech. Memo.*, *NASA TM-89871*, 1–268.

Grant, J. A. (2000), Valley formation in Margaritifer Sinus, Mars, by precipitation-recharged ground-water sapping, *Geology*, *28*, 223–226.

Grant, J. A., and T. J. Parker (2002), Drainage evolution in the Margaritifer Sinus region, Mars, *J. Geophys. Res.*, *107*(E9), 5066, doi:10.1029/2001JE001678.

Grant, J. A., and P. H. Schultz (1990), Gradational epochs on Mars: Evidence from west-northwest of Isidis Basin and Electris, *Icarus*, *84*, 166–195.

Grant, J. A., and P. H. Schultz (1993), Degradation of selected terrestrial and Martian impact craters, *J. Geophys. Res.*, *98*, 11,025–11,042.

Grant, J. A., R. Arvidson, L. S. Crumpler, M. P. Golombek, B. Hahn, A. F. C. Haldemann, R. Li, L. A. Soderblom, S. W. Squyres, and W. A. Watters (2005), Crater gradation in Gusev crater and Meridiani Planum, Mars, *J. Geophys. Res.*, doi:10.1029/2005JE002465, in press.

Greeley, R., and J. E. Guest (1987), Geologic map of the eastern equatorial region of Mars, 1:15,000,000 scale, *U.S. Geol. Surv. Geol. Invest. Ser., Map I-1802-B*.

Greeley, R., and J. D. Iversen (1985), *Wind as a Geological Process*, 333 pp., Cambridge Univ. Press, New York.

Gulick, V. C. (2001), Origin of the valley networks on Mars: A hydrological perspective, *Geomorphology*, *37*, 241–268.

Haberle, R. M. (1998), Early Mars climate models, *J. Geophys. Res.*, *103*, 28,467–28,479.

Hartmann, W. K., and G. Neukum (2001), Cratering chronology and the evolution of Mars, *Space Sci. Rev.*, *96*, 165–194.

Horton, R. E. (1932), Drainage basin characteristics, *Eos Trans. AGU*, *13*, 350–361.

Howard, A. D. (1971), Optimal angles of stream junction: Geometric, stability to capture, and minimum power criteria, *Water Resour. Res.*, *7*, 863–873.

Howard, A. D. (1988), Introduction: Groundwater sapping on Mars and Earth, in *Sapping Features of the Colorado Plateau: A Comparative Planetary Geology Field Guide*, edited by A. D. Howard et al., *NASA Spec. Publ., NASA SP-491*, 1–5.

Howard, A. D., and J. M. Moore (2004), Changing style of erosion during the Noachian-Hesperian transition and a possible climatic optimum, *Proc. Lunar Planet. Sci. Conf. 35th*, Abstract 1192.

Howard, A. D., J. M. Moore, R. A. Craddock, and R. P. Irwin III (2004), Erosional history of the Martian highlands during the Noachian and Hesperian, in *Second Conference on Early Mars*, Abstract 8013, Lunar and Planet. Inst., Houston, Tex.

Howard, A. D., J. M. Moore, and R. P. Irwin III (2005), An intense terminal epoch of widespread fluvial activity in the Martian highlands: 1. Valley network incision and associated deposits, *J. Geophys. Res.*, *110*, E12S14, doi:10.1029/2005JE002459.

Hynek, B. M., and R. J. Phillips (2003), New data reveal mature, integrated drainage systems on Mars indicative of past precipitation, *Geology*, *31*, 757–760.

Irwin, R. P., III, and A. D. Howard (2002), Drainage basin evolution in Noachian Terra Cimmeria, Mars, *J. Geophys. Res.*, *107*(E7), 5056, doi:10.1029/2001JE001818.

Irwin, R. P., III, A. D. Howard, and T. A. Maxwell (2004a), Geomorphology of Ma'adim Vallis, Mars, and associated paleolake basins, *J. Geophys. Res.*, *109*, E12009, doi:10.1029/2004JE002287.

Irwin, R. P., III, T. R. Watters, A. D. Howard, and J. R. Zimbelman (2004b), Sedimentary resurfacing and fretted terrain development along the crustal dichotomy boundary, Aeolis Mensae, Mars, *J. Geophys. Res.*, *109*, E09011, doi:10.1029/2004JE002248.

Irwin, R. P., III, R. A. Craddock, and A. D. Howard (2005), Interior channels in Martian valley networks: Discharge and runoff production, *Geology*, *33*(6), 489–492.

Jankowski, D. G., and S. W. Squyres (1993), "Softened" impact craters on Mars: Implications for ground ice and the structure of the Martian regolith, *Icarus*, *106*, 365–379.

Jerolmack, D. J., D. Mohrig, M. T. Zuber, and S. Byrne (2004), A minimum time for the formation of Holden Northeast fan, Mars, *Geophys. Res. Lett.*, *31*, L21701, doi:10.1029/2004GL021326.

Knighton, D. (1998), *Fluvial Forms and Processes: A New Perspective*, 383 pp., Oxford Univ. Press, New York.

Komar, P. D. (1980), Modes of sediment transport in channelized water flows with ramifications to the erosion of the Martian outflow channels, *Icarus*, *42*, 317–329.

Komatsu, G., and V. R. Baker (1997), Paleohydrology and flood geomorphology of Ares Vallis, *J. Geophys. Res.*, *102*, 4151–4160.

Lanz, J. K., R. Hebenstreit, and R. Jaumann (2000), Martian channels and their geomorphologic development as revealed by MOLA, in *Second Mars Polar Science Conference*, abstract 4026, Lunar and Planet. Inst., Houston, Tex.

Leverington, D. W., and T. A. Maxwell (2004), An igneous origin for features of a candidate crater-lake system in western Memnonia, Mars, *J. Geophys. Res.*, *109*, E06006, doi:10.1029/2004JE002237.

Lucchitta, B. K. (1984), Ice and debris in the fretted terrain, Mars, *Proc. Lunar Planet. Sci. Conf. 14th*, Part 2, *J. Geophys. Res.*, *89*, suppl., B409–B418.

Luo, W. (2002), Hypsometric analysis of Margaritifer Sinus and origin of valley networks, *J. Geophys. Res.*, *107*(E10), 5071, doi:10.1029/2001JE001500.

Maizels, J. (1990), Raised channel systems as indicators of palaeohydrologic change: A case study from Oman, *Palaeogeogr. Palaeoclimatol. Palaeoecol.*, *76*, 241–277.

Malde, H. E. (1968), The catastrophic Late Pleistocene Bonneville Flood in the Snake River Plain, Idaho, *U.S. Geol. Surv. Prof. Pap.*, *596*, 52 pp.

Malin, M. C. (1976), Age of Martian channels, *J. Geophys. Res.*, *81*, 4825–4845.

Malin, M. C., and M. H. Carr (1999), Groundwater formation of Martian valleys, *Nature*, *397*, 589–591.

Malin, M. C., and K. S. Edgett (1999), Oceans or seas in the Martian northern lowlands: High resolution imaging tests of proposed shorelines, *Geophys. Res. Lett.*, *26*, 3049–3052.

Malin, M. C., and K. S. Edgett (2000), Sedimentary rocks of early Mars, *Science*, *290*, 1927–1937.

Malin, M. C., and K. S. Edgett (2003), Evidence for persistent flow and aqueous sedimentation on early Mars, *Science*, *302*, 1931–1934, doi:10.1126/science.1090544.

Mangold, N. (2003), Geomorphic analysis of lobate debris aprons on Mars at Mars Orbiter Camera scale: Evidence for ice sublimation initiated by fractures, *J. Geophys. Res.*, *108*(E4), 8021, doi:10.1029/2002JE001885.

Mangold, N., and V. Ansan (2005), Detailed study of an hydrological system of valleys, delta and lakes in the Southwest Thaumasia region, Mars, *Icarus*, in press.

Mangold, N., C. Quantin, V. Ansan, C. Delacourt, and P. Allemand (2004), Evidence for precipitation on Mars from dendritic valleys in the Valles Marineris area, *Science*, *305*, 78–81.

Mars Channel Working Group (1983), Channels and valleys on Mars, *Geol. Soc. Am. Bull.*, *94*, 1035–1054.

Masursky, H., J. M. Boyce, A. L. Dial, G. G. Schaber, and M. E. Strobell (1977), Classification and time of formation of Martian channels based on Viking data, *J. Geophys. Res.*, *82*, 4016–4038.

Maxwell, T. A., and G. E. McGill (1988), Ages of fracturing and resurfacing in the Amenthes region, Mars, *Proc. Lunar Planet Sci. Conf. 18th*, 701–711.

McGill, G. E. (2000), Crustal history of north central Arabia Terra, Mars, *J. Geophys. Res.*, *105*(E3), 6945–6960.

McGill, G. E. (2002), Geologic map transecting the highland/lowland boundary zone, Arabia Terra, Mars: Quadrangles 30332, 35332, 40332, and 45332, scale 1:1M, *U.S. Geol. Surv. Geol. Invest. Ser., Map I-2746*.

Milton, D. J. (1973), Water and processes of degradation in the Martian landscape, *J. Geophys. Res.*, *78*, 4037–4047.

Moore, J. M., and A. D. Howard (2005), Large alluvial fans on Mars, *J. Geophys. Res.*, *110*, E04005, doi:10.1029/2004JE002352.

Moore, J. M., A. D. Howard, W. E. Dietrich, and P. M. Schenk (2003), Martian layered fluvial deposits: Implications for Noachian climate scenarios, *Geophys. Res. Lett.*, *30*(24), 2292, doi:10.1029/2003GL019002.

Nanson, G. C., and J. C. Croke (1992), A genetic classification of floodplains, *Geomorphology*, *4*, 459–486.

Neukum, G., and K. Hiller (1981), Martian ages, *J. Geophys. Res.*, *86*, 3097–3121.

Öpik, E. J. (1966), The Martian surface, *Science*, *153*, 255–265.

Ori, G. G., L. Marinangeli, and A. Baliva (2000), Terraces and Gilbert-type deltas in crater lakes in Ismenius Lacus and Memnonia (Mars), *J. Geophys. Res.*, *105*, 17,629–17,641.

Osterkamp, W. R., and E. R. Hedman (1982), Perennial-streamflow characteristics related to channel geometry and sediment in Missouri River basin, *U.S. Geol. Surv. Prof. Pap.*, *1242*, 37 pp.

Pelkey, S. M., and B. M. Jakosky (2002), Surficial geologic surveys of Gale Crater and Melas Chasma, Mars: Integration of remote-sensing data, *Icarus*, *160*, 228–257.

Pelkey, S. M., B. M. Jakosky, and P. R. Christensen (2004), Surficial properties in Gale Crater, Mars, from Mars Odyssey THEMIS data, *Icarus*, *167*, 244–270.

Phillips, R. J., M. T. Zuber, S. C. Solomon, M. P. Golombek, B. M. Jakosky, W. B. Banerdt, R. M. E. Williams, B. M. Hynek, O. Aharonson, and S. A. Hauck II (2001), Ancient geodynamics and global-scale hydrology on Mars, *Science*, *291*, 2587–2591.

Pieri, D. C. (1980), Geomorphology of Martian valleys, in *Advances in Planetary Geology*, *NASA Tech. Memo.*, *NASA TM-81979*, 1–160.

Pondrelli, M., A. Baliva, S. Di Lorenzo, L. Marinangeli, and A. P. Rossi (2005), Complex evolution of paleolacustrine systems on Mars: An example from the Holden crater, *J. Geophys. Res.*, *110*, E04016, doi:10.1029/2004JE002335.

Ritter, D. F., R. C. Kochel, and J. R. Miller (1995), *Process Geomorphology*, 3rd ed., 560 pp., McGraw-Hill, New York.
Sagan, C., O. B. Toon, and P. J. Gierasch (1973), Climate change on Mars, *Science*, *181*, 1045–1049.
Scott, D. H., and M. G. Chapman (1995), Geologic and topographic maps of the Elysium paleolake basin, Mars, scale 1:5M, *U.S. Geol. Surv. Geol. Invest. Ser., Map I-2397*.
Scott, D. H., E. C. Morris, and M. N. West (1978), Geologic map of the Aeolis quadrangle of Mars, scale 1:5M, *U.S. Geol. Surv. Misc. Invest. Ser., Map I-1111*.
Segura, T. L., O. B. Toon, A. Colaprete, and K. Zahnle (2002), Environmental impacts of large impacts on Mars, *Science*, *298*, 1977–1980.
Squyres, S. W. (1978), Martian fretted terrain: Flow of erosional debris, *Icarus*, *34*, 600–613.
Squyres, S. W., and J. F. Kasting (1994), Early Mars: How warm and how wet?, *Science*, *265*, 744–749.
Squyres, S. W., et al. (2004), In situ evidence for an ancient aqueous environment at Meridiani Planum, Mars, *Science*, *306*, 1709–1714.
Stepinski, T. F., and M. L. Collier (2004), Extraction of Martian valley networks from digital topography, *J. Geophys. Res.*, *109*, E11005, doi:10.1029/2004JE002269.
Stepinski, T. F., and S. Coradetti (2004), Comparing morphologies of drainage basins on Mars and Earth using integral-geometry and neural maps, *Geophys. Res. Lett.*, *31*, L15604, doi:10.1029/2004GL020359.
Stepinski, T. F., M. L. Collier, P. J. McGovern, and S. M. Clifford (2004), Martian geomorphology from fractal analysis of drainage networks, *J. Geophys. Res.*, *109*, E02005, doi:10.1029/2003JE002098.
Strom, R. G., S. K. Croft, and N. D. Barlow (1992), The Martian impact cratering record, in *Mars*, edited by H. H. Kieffer et al., pp. 383–423, Univ. of Ariz. Press, Tucson.
Tanaka, K. L. (1986), The stratigraphy of Mars, *Proc. Lunar Planet. Sci. Conf. 17th*, Part 1, *J. Geophys. Res.*, *91*, suppl., E139–E158.
Tanaka, K. L., J. A. Skinner Jr., T. M. Hare, T. Joyal, and A. Wenker (2003), Resurfacing history of the northern plains of Mars based on geologic mapping of Mars Global Surveyor data, *J. Geophys. Res.*, *108*(E4), 8043, doi:10.1029/2002JE001908.
Trenhaile, A. S. (2001), Modelling the Quaternary evolution of shore platforms and erosional coastal shelves, *Earth Surf. Processes Landforms*, *26*, 1103–1128.
Trenhaile, A. S. (2002), Modeling the development of marine terraces on tectonically mobile rock coasts, *Mar. Geol.*, *185*, 341–361.
Weitz, C. M., M. C. Bourke, F. C. Chuang, and D. A. Crown (2004), An unusual lobate deposit in Coprates Catena, Mars, *Eos Trans. AGU*, *85*(47), Fall Meet. Suppl., Abstract P13A-0989.
Whitmire, D. P., L. R. Doyle, R. T. Reynolds, and J. J. Matese (1995), A slightly more massive young Sun as an explanation for warm temperatures on early Mars, *J. Geophys. Res.*, *100*, 5457–5464.
Williams, R. M. E., and K. S. Edgett (2005), Valleys in the Martian rock record, *Proc. Lunar Planet. Sci. Conf. 36th*, abstract 1099.
Williams, R. M. E., K. S. Edgett, and M. C. Malin (2004), Young fans in an equatorial crater in Xanthe Terra, Mars, *Proc. Lunar Planet. Sci. Conf. 35th*, abstract 1415.
Williams, R. M. E., M. C. Malin, and K. S. Edgett (2005), Remnants of the courses of fine-scale, precipitation-fed runoff streams preserved in the Martian rock record, *Proc. Lunar Planet. Sci. Conf. 36th*, abstract 1173.

R. A. Craddock and R. P. Irwin III, Center for Earth and Planetary Studies, National Air and Space Museum, Smithsonian Institution, 6th Street and Independence Avenue SW, Washington, DC 20013-7012, USA. (irwinr@si.edu)

A. D. Howard, Department of Environmental Sciences, University of Virginia, P.O. Box 400123, Charlottesville, VA 22904-4123, USA. (ah6p@virginia.edu)

J. M. Moore, Space Sciences Division, NASA Ames Research Center, MS 245-3, Moffett Field, CA 94035, USA. (jeff.moore@nasa.gov)